2013

CERIUM OXIDE (CeO2) PROMOTED OXYGEN CARRIER DEVELOPMENT AND SCALE MODELING STUDY FOR CHEMICAL LOOPING COMBUSTION

Fang Liu
University of Kentucky, liufangcumt@gmail.com

STUDENT AGREEMENT:

I represent that my thesis or dissertation and abstract are my original work. Proper attribution has been given to all outside sources. I understand that I am solely responsible for obtaining any needed copyright permissions. I have obtained and attached hereto needed written permission statements(s) from the owner(s) of each third-party copyrighted matter to be included in my work, allowing electronic distribution (if such use is not permitted by the fair use doctrine).

I hereby grant to The University of Kentucky and its agents the non-exclusive license to archive and make accessible my work in whole or in part in all forms of media, now or hereafter known. I agree that the document mentioned above may be made available immediately for worldwide access unless a preapproved embargo applies.

I retain all other ownership rights to the copyright of my work. I also retain the right to use in future works (such as articles or books) all or part of my work. I understand that I am free to register the copyright to my work.

REVIEW, APPROVAL AND ACCEPTANCE

The document mentioned above has been reviewed and accepted by the student's advisor, on behalf of the advisory committee, and by the Director of Graduate Studies (DGS), on behalf of the program; we verify that this is the final, approved version of the student's dissertation including all changes required by the advisory committee. The undersigned agree to abide by the statements above.

Fang Liu, Student

Dr. Kozo Saito, Major Professor

Dr. James McDonough, Director of Graduate Studies

CERIUM OXIDE (CeO_2) PROMOTED OXYGEN CARRIER DEVELOPMENT AND SCALE MODELING STUDY FOR CHEMICAL LOOPING COMBUSTION

DISSERTATION

A dissertation submitted in partial fulfillment of the
requirement for the degree of Doctor of Philosophy in the
College of Engineering
at the University of Kentucky

By
Fang Liu
Lexington, Kentucky
Director: Dr. Kozo Saito, Professor of Mechanical Engineering
Lexington, Kentucky
2013

ABSTRACT OF DISSERTATION

CERIUM OXIDE (CeO_2) PROMOTED OXYGEN CARRIER DEVELOPMENT AND SCALE MODELING STUDY FOR CHEMICAL LOOPING COMBUSTION

According to IPCC reports, the greenhouse gas CO_2 is responsible for global climate change. Studies show that CO_2 concentration reached a level of 400 ppm in 2013, or 40 % above pre-industrial levels. The contribution of CO_2 from industrial activity to increasing global CO_2 concentrations is widely accepted and points to the need to reduce the emission of this greenhouse gas. One possible combustion technology that shows promise for reducing CO_2 emissions is chemical looping combustion (CLC). It is an oxy-fuel technology, but has the advantages of *in situ* oxygen separation, low NO_x emissions and low cost of CO_2 emission abatement; it entails the use of an oxygen carrier (OC) to provide oxygen for combusting fuels.

OC development is an important task in CLC. Iron based OCs have attracted most research attention in recent years, mainly due to their inexpensive and non-toxic nature. Bi-metal oxide OCs usually impart better CLC performance than mono-metal oxide OCs, one example of which is the introduction of CeO_2 as a partially reducible material capable of generating oxygen vacancies that lead to oxygen storage and transfer. In this study, CeO_2 was used as an additive to a Fe_2O_3-based OC and its effect on physical properties, such as morphology, surface area and mechanical strength, was analyzed in detail. The reactivity of OCs is studied using TGA-MS and a bench scale CLC setup. The results show that the reduction reaction at the surface is independent of whether CeO_2 is present or not, but after the surface oxygen had been consumed, the OC with CeO_2 provided faster oxygen transfer rates from the bulk to the surface to produce better average reaction rates. The OCs after reduction and oxidation were analyzed using XRD and Raman spectroscopy; based on these analytical data, a model for the promoting role of CeO_2 is discussed. Furthermore, the reaction kinetics of the OCs were also studied using shrinking core model, the kinetics parameters were obtained and compared.

Scale-up of laboratory-scale CLC reactors is another important task necessary to develop an understanding of the potential and efficiencies of CLC. In this study, scaling laws were used as a guide to design and then build two different-sized CLC reactors. Testing of the reactors involved a focus on chemical similarities. Comparisons of the performance of both reactors showed good consistency, thereby validating the scale modeling method and the scale laws for CLC reactors.

KEYWORDS: Oxygen Carrier, Reactivity; Diffusion Mechanism; Solid Solution, Scale-up

Fang Liu

Student's Signature

December 18, 2013

Date

CERIUM OXIDE (CeO_2) PROMOTED OXYGEN CARRIER DEVELOPMENT AND SCALE MODELING STUDY FOR CHEMICAL LOOPING COMBUSTION

By

Fang Liu

Prof. Kozo Saito
Director of Dissertation

Prof. James McDonough
Director of Graduate Studies

December 18, 2013

Acknowledgments

Completing this dissertation has required help from a great many people; I am deeply grateful to all of them. I have benefited personally and professionally through their kind help and support, and they have made my graduate study experience one that I will cherish forever.

First, I would like to thank Dr. Kunlei Liu and Dr. Kozo Saito for enabling me to study and perform my PhD dissertation at the University of Kentucky. Their patience and support helped me overcome some difficulties and provided guidance for completing this dissertation. I am grateful to Dr. Kunlei Liu for his insightful instructions, encouragement and financial support. He is an excellent example from whom I learned how to do quality research, and of the importance of the attitudes of seriousness and dedication that are necessary for accomplishing goals in research and life. My advisor Dr. Kozo Saito has also been an excellent example, one who always trusted and encouraged us. His teaching and encouragement were and are inspiring, and I thank him for the guidance in scale modeling for this dissertation.

Second, I am thankful to my co-advisor Dr. James K. Neathery, who gave me the freedom to explore ideas and concepts on my own. I am also thankful to him for encouraging the use of correct grammar and consistent notation in my writings.

Third, I would like to thank my committee members, Dr. Lawrence Holloway, Dr. Thomas Lester, Dr. Tingwen Wu, Dr. Tianxiang Li and Dr. Ruigang Yang for reviewing my dissertation, for their alternative ideas and explanations which have undoubtedly augmented this work, and for their timely flexibility.

Fourth, I am also grateful to people who have helped to make this dissertation better. Special thanks to Dr. John Stencel, Dr. Qiying Jiang, Dr. Yi Zhang, Dr. Liangyong Chen, Dr. James Landon and Mrs. Lisa Richburg who gave insightful comments and constructive criticism on how to improve the dissertation. I want to thank Dr. Dali Qian for the help on SEM imaging, and Dr. Xin Gao for measurement of BET surface areas. I also would like to acknowledge Dr. Gary Jacobs and Dr. Yaying Ji for numerous discussions on related topics that helped me improve my knowledge in the area.

Fifth, I acknowledge and appreciate the financial support from Carbon Management Research Group (CMRG) at the Center for Applied Energy Research of the University of Kentucky.

Finally, and most importantly, I would like to thank my wife Li Yang for her love, understanding and dedication to our family. And, to my little daughter Alice, I take great pleasure in playing with you after each day of research and work. I am also indebted to my parents for their encouragement and support.

Table of Content

List of Tables

List of Figures

1. Introduction

1.1 Background

In recent years, as the issues associated with atmospheric chemistry and the potential of global warming has come into focus, professional, industrial, governmental and private organizations and panels have conducted research to examine and expound future global weather scenarios that are based on well-founded theories, experiments and data. To date, a general consensus has been formed on how climate is changing and may further change into the future. It is known that the average earth surface temperature and sea levels are increasing while snow cover is decreasing; it is projected that the average temperature will continue to rise at a rapid rate [1].

Greenhouse gases (GHG), such as water vapor (H_2O), carbon dioxide (CO_2), methane (CH_4) and ozone (O_3), have been established as main atmospheric constituents that can drive global warming, with CO_2 the most prevalent, and the most affected by human activity and industry [2]. Studies show that atmospheric CO_2 concentrations reached 400 ppm in 2013 [3-5] , or 40 % above pre-industrial levels. CO_2 emitted into the atmosphere by fossil fuel combustion is the most significant greenhouse gas contributing to climate change, and the use of coal alone accounted for 43 % of global CO_2 emission in 2010 [6]. The influence of CO_2 from industrial activity on increasing global CO_2 concentrations is widely accepted and points to the need to reduce emissions of this greenhouse gas. However, the number of options that could be employed to mitigate increases in CO_2 atmospheric levels is limited and will need to include both CO_2 capture and its storage.

1.2 CO_2 capture and disposal

Currently, three main technologies for CO_2 capture from power production have been examined: post-combustion, pre-combustion, and oxy-fuel combustion. In post-combustion technologies the CO_2 is captured from the flue gas after combustion of the fuel, and usually involves a two-step process that employs separation and regeneration technologies. During CO_2 separation from the flue gas, absorption, adsorption, and membrane or cryogenic processes could be employed [7]. Then, regeneration of the separation medium is used to release the captured CO_2 and to recycle the capture medium for re-use in CO_2 separation. However, typical CO_2 concentrations in flue gas for post-combustion processes are lower than 15 %; hence, the thermodynamic driving force for CO_2 capture is low and the costs are high [8]. As an example, the energy required for CO_2 capture using monoethanolamine (MEA) is estimated to reduce a pulverized coal combustion plant's output by about 30 % , which would equate to a very substantial 80% increase in the cost of electricity [9].

Pre-combustion processing is usually applied to integrated gasification combined cycle (IGCC) using gas-liquid absorption [10]. The first step is to partially oxidize a fuel containing carbon and hydrogen to H_2 and CO. Steam is then injected into the reaction zone to induce the water-gas-shift reaction: $CO+H_2O \rightarrow CO_2+H_2$, converting CO into CO_2 and generating high concentrations of H_2 which is a fuel having low greenhouse gas emission potential. The CO_2 is then separated using methods very similar to those used in post-combustion processing. However, CO_2 capture by pre-combustion processing is not

technically easy or inexpensive. For example, the energy penalty for pre-combustion CO_2 capture was calculated to be 18 %-19 % [11].

Oxy-fuel combustion uses pure oxygen to combust fuels, and produces flue gas containing primarily CO_2 and water vapor. Water vapor is very easy to condense, resulting in a pure CO_2 stream which is ready to capture. However, an air separation unit (ASU) is required in oxy-fuel combustion to provide pure oxygen separated from air, and is a high-energy consuming process [12]. An alternative is to use a solid metal oxide as an oxygen carrier (OC). The method that adopts metal oxides to provide oxygen for oxy-fuel combustion is known as chemical looping combustion (CLC).

For all technologies to be used for CO_2 capture, it is necessary to compress the CO_2 under high pressure for sequestration or further use. The CO_2 can be used as a raw material in food production, firefighting, fish farming, and rubber and plastic processing, etc [2]. It can also been used to promote crude oil and natural gas production by injection into wells, helping to drive the crude oil and natural gas to surface processing equipment [13]. But the amount of CO_2 used by these types of industrial activity is very small relative to the vast amount generated during power production from hydrocarbon fuels [14]. It would therefore be necessary, if CO_2 capture technologies are employed for mitigating greenhouse gas emissions, to transport huge amounts and then to store it in secure and isolated underground locations for 100's-to-1,000's of years. Alternative to storage of CO_2 in geological formations, it may also be possible to store it through surface mineral carbonation or underwater. However, in all possible scenarios, the location and approach

must be thoroughly investigated before implementation because CO_2 leakage can seriously hurt people, damage property, make seawater more acidic and threaten sea animals and plant life.

Therefore, widespread, highly efficient and safe CO_2 emission abatement and storage technologies would be required for future control of atmospheric CO_2 concentration or mitigation of its emission during industrial processing. The task is daunting. Nevertheless, this dissertation examines a small but important segment of a promising approach for CO_2 capture from flue gas – chemical looping combustion (CLC).

1.3 Chemical looping combustion introduction

Among CO_2 capture technologies, CLC has been proposed to be one offering higher efficiencies and lower costs [15-16]. It is a type of oxy-fuel combustion having the advantage of *in situ* oxygen separability and low NO_x emissions. In other words, CO_2 can be separated from flue gas inherently without the use of an energy-intensive, external ASU that is required for conventional oxy-fuel technology. Accordingly, CLC technology, as depicted in Figure 1, may be a promising method for fossil-based power generation in a carbon-constrained world.

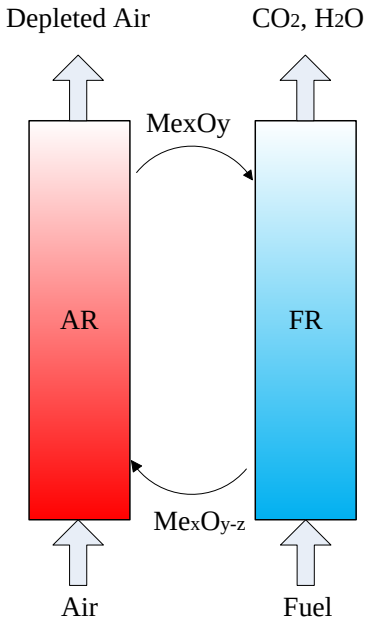

Figure 1 Ideal CLC diagram.

CLC uses a solid oxygen carrier (OC), usually a metal oxide, to provide oxygen for combusting fuel without the presence of nitrogen from air. The reduced OC is then recycled to an air reactor (AR) to be re-oxidized, and then it is re-used in the fuel reactor (FR) to provide oxygen in subsequent fuel combustion cycles. Through the use of the OC, the flue gas is separated into two parts. The air reactor gas outlet contains a high–temperature, oxygen-depleted gas containing mostly N_2. The fuel reactor outlet gas is primarily water vapor and CO_2. Because water vapor can be condensed very easily, an exhaust gas can be made that is highly concentrated in CO_2 and readied for compression and storage.

The reactions in the fuel reactor and the air reactor can be expressed as:

Fuel reactor:

$$\frac{1}{z}\left(2m+\frac{n}{2}\right)Me_xO_y + C_mH_n \rightarrow \frac{1}{z}(2m+\frac{n}{2})Me_xO_{y-z} + mCO_2 + \frac{n}{2}H_2O \qquad (1)$$

Air reactor:

$$Me_xO_{y-z} + \frac{1}{2}zO_2 \rightarrow Me_xO_y \quad (2)$$

The overall reaction is:

$$C_mH_n + \left(m + \frac{1}{4}n\right)O_2 \rightarrow mCO_2 + \frac{1}{2}nH_2O \quad (3)$$

1.4 CLC combined power generation

CLC technology is suited for power generation because the flue gas from the air reactor is at high temperatures as is the flue gas from the fuel reactor [17]. Hence, gas and CO_2 turbines can be used to generate power.

Recent studies have shown that CLC with CO_2 capture would have higher efficiency than traditional pulverized coal (PC) power generation under similar conditions [18-23]. According to a Department of Energy (D.O.E) report [24], a CLC-based CO_2 capture system could give higher overall efficiency than that of post-combustion CO_2 capture or alternative oxy-fuel technologies. A pressurized CLC, super-critical power plant would have the highest efficiency up to 46 %, which is almost double that achieved in sub-critical PC plants equipped with an amine scrubber (~25 % efficiency) or of an oxy-fuel PC system (~27 %), and is about 50 % greater than that of a state-of-the-art IGCC providing CO_2 enrichment (36 % efficiency). Naqvi et. al. [19] designed a detailed CLC power generation plant using natural gas as fuel, and analyzed the thermodynamic cycle of this plant based on a steady state model. Their results show that a CLC power generation plant could achieve an overall efficiency of 49.7 % with zero CO_2 emissions.

With such advantages, CLC has attracted intensive attention in the last decade, with bench scale and pilot scale testing successfully showing the feasibility of CLC processing

using various OC's and fuels. However, CLC technology still has a long way to go before being applied commercially. One of the main bottlenecks is the OC itself because excellent reactivity and stability are required for overall economic viability of CLC processing [2, 17]. Furthermore, appropriate methods for reactor scale-up also need to be figured out.

2. Literature Review

2.1 Oxygen carrier introduction

Since the beginning of CLC research, OC development has always been a key focus of study due to the concern of slow reaction rates in the fuel reactor. Active metal oxides would rapidly provide oxygen during the reduction reaction, and re-obtain oxygen during oxidation in the air reactor, hence the name oxygen carrier (OC). The transition metals, such as Ni, Co, Cu, and Fe, have several different valence states; they are usually used as OCs. The performance of OCs is a key point for successful CLC processing, the requirements of which can be described as:

(1). High oxygen transfer capacity and high reaction rate;

(2). High stability/durability;

(3). Good mechanical strength and low attrition rate;

(4). Cost-effective and environmentally acceptable.

The OCs can be produced using several different methods, with freeze granulation, impregnation and spray-drying the most popular [8, 25-31]. The OCs produced by these methods are usually called synthetic OCs in contrast to natural OCs from, for example, ilmenite ($FeTiO_3$) which can be used after crushing mined ores; typically, natural OCs are less expensive than synthetic OCs. For synthetic OCs, inert materials like Al_2O_3, SiO_2, TiO_2, YSZ and ZrO_2 are usually used as supports for the active transition metal oxides. The support works as a binder to increase the mechanical strength and helps to disperse the metal oxide which enables increased surface areas. Hence, the reactivity and durability of OCs can be enhanced by using support materials.

2.2 Performance evaluation

The performance of OCs is evaluated using the following parameters and methods.

(1) Oxygen transport capacity, R_o

The oxygen transport capacity, R_o, is an important property of OCs, and is defined as the mass fraction of usable oxygen in the OCs between the air reactor and fuel reactor:

$$R_o = (m_{ox} - m_{red})/m_{ox} \times 100\ \% \quad (4)$$

where m_{ox} is the mass of the OC in an oxidized state in grams and m_{red} is the mass of the OC in its reduced state in grams.

The oxygen transport capacity of several metal oxides is listed in Figure 2. The CuO, NiO and CoO have relative higher oxygen transfer capacities; however, Fe_2O_3 has the highest theoretical oxygen transfer capacity. If Fe_2O_3 was reduced to metallic iron (Fe), it would have an oxygen transport capacity of 30 %.

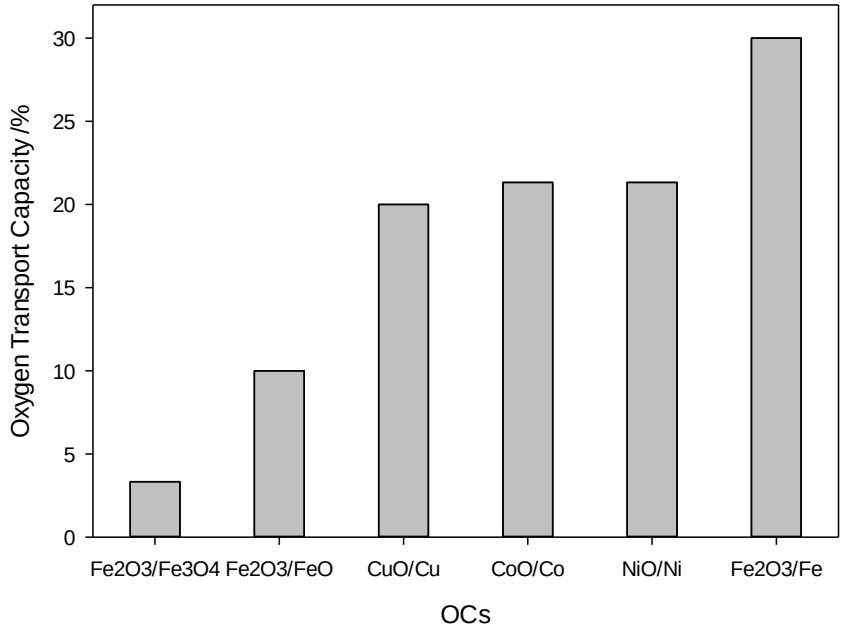

Figure 2 Theoretical oxygen transfer capacity.

(2) Conversion of reduction, X_r, and reaction rate, w

Conversion of reduction is the degree of OC reduction, and can be defined as the actual mass loss of OC divided by the mass of oxygen that the OC could provide:

$$X_r = (m_{ox} - m)/(m_{ox} - m_{red}) \times 100\ \% \quad (5)$$

The reaction rate w is defined by time rate of change of conversion:

$$w = dX_r/dt \quad (6)$$

(3) Mechanical strength

Mechanical strength reflects, to some degree, the particles resistance to attrition stresses. Particles with higher mechanical strength possess a higher ability to retain their initial shape, and thus would exhibit better durability. It is worth noting that, for the OC mechanical strength to be comparable in a study, a narrow particle size distribution must be used.

2.3 OC screening

In the last two decades, a number of institutes have begun working in OC development research; Table 1 lists the major affiliations of these institutes and their OC product. Most of the OCs are synthetic, with NiO, CuO or Fe_2O_3 as the active metal oxides. Natural OCs such as ilmenite ($FeTiO_3$) have also been studied. The OCs were investigated in TGA or bench scale reactors using varies fuels.

Fan [32] compared the performance of NiO, CuO and Fe_2O_3 based OCs, as shown in Table 2. Nickel based OCs have the advantage of fast reaction rates and a fair melting point, however, nickel oxides lack mechanical strength and are toxic to humans and the environment. Copper oxides also show high reactivity, but tend to agglomerate [27]. Iron

based OCs have attracted most research attention in recent years, mainly due to their inexpensive and non-toxic nature, they also have sufficient reaction rates. The advantages of low cost and high mechanical strength of iron based OCs led to their use in a commercial CLC project [2, 26, 33]. Our recent study showed that, in comparison to the other two metal oxides (NiO and CuO), Fe_2O_3 based OCs exhibited much better resistance to water vapor degradation [34]. Hence, Fe_2O_3 is currently believed to be the most suitable material for OC development.

2.4 Thermodynamic analysis

The reaction in the fuel reactor is reduction, which can be endothermic or exothermic. The reaction in the air reactor is oxidation, usually exothermic. With Fe_2O_3, the reactions in a CLC using gaseous fuels such as CO and oxidants (O_2) are listed in Table 3. Fe_2O_3 can be reduced to Fe_3O_4, FeO and even the metallic iron (Fe) depending on the degree of reduction [35].

The heat of reaction (in this case, heat of combustion) can be calculated from: [36]

$$\Delta H(T^O) = \sum_i (v_i^{"} - v_i^{'}) H_i^o (T^O) \quad (7)$$

Where:

ΔH is heat of reaction, kJ mol^{-1};

$v_i^{"}$ is mole concentration coefficient of product;

$v_i^{'}$ is mole concentration coefficient of reactant;

H_i^o is heat of formation, kJ mol^{-1}.

The heat of combustion for related reactions is also listed in Table 3. Most of these reactions are exothermal, which is beneficial when designing the reactor because less external-supplied thermal energy would be needed in the fuel reactor.

Table 1 CLC research institutes and the OCs

Institute	Researchers	OCs (active metals)	Fuel
Tokyo Institute of Technology	Nakano, Ishida, Jin, Okamoto	NiO, Fe_2O_3	H_2, CO, CH_4
Chalmers University of Technology	Lyngfelt, Zafar Mattisson, Johansson, Leion,	NiO, Fe_2O_3, CuO, Ilmenite, Hematite, Sandvik,	natural gas, CH_4, syngas, petroleum coke, charcoal,
Institute de Carboquimica	Abad, de Diego, Beatriz	NiO, Fe_2O_3, CuO, Ilmenite,	natural gas, CH_4, syngas
Ohio State University	Fan	Fe_2O_3	solid fuel
Korea Institute of Technology	Son	Fe_2O_3	CH_4
Southeast University	Xiao, Gu	$CaSO_4$, Fe_2O_3	syngas, coal
Technical University of Viena	Kolbitsch	NiO, CoO	CH_4, syngas
Alstom	Andrus	$CaSO_4$	Coal
University of Kentucky	Kunlei Liu	Fe_2O_3, Ilmenite	CO, syngas, coal char

Table 2 Comparison of Ni, Cu and Fe- based OCs

OC	Ni- based	Cu- based	Fe- based
Reactivity	good	good	low
Melting point	fair	low	high
Strength	low	fair	good
Toxic	yes	no	no
Cost	high	high	low

Table 3 Reactions and heat of combustion

Reaction	Heat of Combustion ΔH (kJ/mol fuel)
$3Fe_2O_3+CO=2Fe_3O_4+CO_2$	-48.3
$Fe_2O_3+CO=2FeO+CO_2$	-1.5
$Fe_2O_3+3CO=2Fe+3CO_2$	7.8
$4Fe_3O_4+O_2=6Fe_2O_3$	-117.4
$4FeO+O_2=2Fe_2O_3$	-140.8
$4Fe+3O_2=2Fe_2O_3$	-412.3

*Heat of formation can be found in NIST-JANAF Thermochemical Tables.[37]

2.5 Iron oxide based OC review

Natural iron oxide OCs such as hematite have low cost and are easily mined and processed; their reactivities have been studied by several researchers [25-26, 38-41]. The results showed they were suitable as OCs in CLC, but the ores had a tendency to agglomerate at high temperature [2], which is problematic for CLC applications. Another possibly important natural OC ore is the ilmenite. It is cheap, abundant and shows good reactivity and oxygen transport capacity [42-47]. It is also recommended to pre-calcine the fresh ilmenite which increases its porosity and mechanical strength. However, a possible disadvantage of it is that defluidization (agglomeration) may occur when the particles are in a highly reduced state [48-49].

Synthetic OCs like Fe_2O_3 supported on Al_2O_3 has been studied in some research. They show good reactivity and mechanical strength, and are better than Fe_2O_3 on TiO_2 and kaolin [8, 30, 50]. Although Fe_2O_3 on Al_2O_3 shows some good properties, it also has some disadvantages. The first one is its tendency to agglomerate [27, 50]. Another disadvantage is that Fe_2O_3 will react with the Al_2O_3 support and form $FeAlO_4$ [2]; this molecular form has decreased oxygen transfer ability.

To avoid the formation of iron aluminate, $MgAl_2O_4$ has also been investigated as a support material; it is a beneficial support because the MgO in the Al_2O_3 eliminates interactions between the iron oxide and the support and helps to maintain the iron oxides' reactivity and durability. Johansson et al [51] studied Fe_2O_3 on $MgAl_2O_4$ in a fluidized bed and examined the influence on OC properties. Their preparation included freeze granulation methods and they used a reductive gas which was 50 vol. % CH_4 balanced

with H_2O. The results showed an optimum OC composition was 60 wt. % Fe_2O_3 and 40 wt. % $MgAl_2O_4$, and when sintered at 1100 ^oC; it had high reactivity and was not easily agglomerated or attritted. Leion et al [49, 52] continued to test this OC using petroleum coke as fuel in a small lab reactor, and showed that the OC reacted quickly with intermediate gasification products such as CO and H_2; the addition of the OC greatly enhanced coke gasification. Zafar et al [29] compared the redox reactivity of Ni, Cu, Fe and Mn supported on SiO_2 and $MgAl_2O_4$, and concluded that Fe on SiO_2 was not a feasible OC because of silicate formation, whereas Fe_2O_3 supported on $MgAl_2O_4$ showed high reactivity.

It has been shown that bi-metal oxide OCs usually work better than mono metal oxide OCs [53]. For example, Johansson et al [53] studied synergistic effects of mixed oxides of nickel oxide, 60 wt. % NiO and 40 wt. % $MgAl_2O_4$ sintered at 1400 ^oC (labeled as N6AM1400), and iron oxide, 60 wt. % Fe_2O_3 and 40 wt. % $MgAl_2O_4$ sintered at 1100 ^oC (F6AM1100). They used 3 wt. % nickel oxide mixed with 97 wt. % iron oxide and conducted tests using a laboratory-scale fluidized bed of quartz with methane as the fuel. The results showed that the CO_2 production rate was twice as much as the sum of the CO_2 production rates when the two oxygen carriers were tested separately. Rydén, et al. [54] did similar experiments using a batch fluidized bed reactor and a circulating fluidized bed reactor, with additives of N6AM1400 or N18-α-Al_2O_3 (18 wt. % NiO supported on Al_2O_3) to ilmenite with different concentrations; the results were that a small amount of nickel oxide added to natural ilmenite increased the overall activity greatly.

Compared to NiO, CuO- based OCs, Fe_2O_3-based OCs are known to have relatively lower reactivity [27, 55]. However, iron oxide is more abundant and less costly, and is non-

toxic [56], and could become more advantageous than these other oxides for commercial scale use if its reactivity could be enhanced. OCs with bi-metal oxide compositions have been shown to be more effective than mono-metal oxides. For example, recent studies have shown the attributes of mixed metal oxide OCs, including: CoO and NiO supported on Al_2O_3 [57]; CuO and NiO supported on Al_2O_3 [58]; Fe_2O_3 and NiO supported on Al_2O_3 or $MgAl_2O_4$ [30, 53]; Fe_2O_3 and MnO_2 without support or supported on ZrO_2 [59-61]; and Fe_2O_3 and CuO supported on Al_2O_3 [62-64]. Compared with these mixed metal oxides, CeO_2 as an additive to OCs has not been extensively studied even though it may impart unique characteristics to iron oxide based OCs.

CeO_2 has a fluorite structure, with each Ce^{4+} surrounded by eight equivalent, nearest O^{2-} ions that form the corners of a cube and coordinated to four Ce^{4+} ions [65]. When the Ce^{4+} ions are replaced by lower valence cations, oxygen vacancies will be created [66]. If two cerium ions are replaced by trivalent ions - for example, by two trivalent Ce^{3+}, an oxygen vacancy or lattice defect is created that can be the most reactive site on the surface of the metal oxide [67]. Both surface and bulk oxygen vacancies occur in CeO_2 and are suitable sites for adsorption [68]. Hence, besides being useful as a support for catalytic surfaces, CeO_2 also can actively participate in chemical reactions.

CeO_2-containing OCs have shown promising results in CLC testing [69-72], in CH_4 reforming for H_2 and CO production [73-77] (chemical looping reforming), and in CO_2 splitting [78-79]. Miller et al [72] added 5 wt. % CeO_2 to hematite (Fe_2O_3) and found improved OC performance for CH_4 oxidation; the CeO_2 did not affect the surface area of the hematite. Li et al [76] used Fe_2O_3 and CeO_2 materials (Fe : Ce molar ratio =3:7) during the conversion of CH_4 to synthesis gas and reported that Fe_2O_3 and CeO_2 formed a solid

solution having higher activity and selectivity than hematite by itself. Galvita et al [79] investigated the effect of CeO_2 upon Fe_2O_3 during H_2-CO_2 redox reactions for CO_2 utilization and found enhanced reaction capacity and increased stability relative to Fe_2O_3 by itself. However, the mechanism by which CeO_2 promotes Fe_2O_3-based OCs during CLC is still not clear. Miller et al [72] theorized that CH_4 first reacted with CeO_2 lattice oxygen to form CO and H_2, and then the reduced cerium oxide promoted CH_4 decomposition to active intermediates such as C and H_2 which, in turn, facilitated a greater use of oxygen from the natural ore hematite. Galvita et al [79], on the other hand, attributed the promotional role of CeO_2 to that of suppressing the sintering of iron oxide. Hence, significant differences currently exist on the promotional role of CeO_2.

No standard exists to evaluate the performance of OCs. Liu et al [35] recommended the the use of FG Fe_2O_3 50 OC (freeze granulated OC with the composition of 50 wt. % Fe_2O_3 and 50 wt. % Al_2O_3) as a reference because it has been very widely studied and has a moderate Fe_2O_3 concentration. It has demonstrated a reasonable reactivity in the presence of water vapor and CO_2, was not highly deactivated due to coal impurities, has high mechanical resistance to attrition, and is cost effective for production. This OC is used as a reference in this dissertation.

2.6 Scale modeling

Reactor scale-up is a major task for engineers and is a fundamental step in the realization and optimization of industrial plants [80]. Scale-up is able to transfer information from equipment of one size to other similar equipment having a different size [81]. Kuwana et al [82] gave an example of understanding phenomena happening in a real process by doing a scale modeling study of a laboratory setup. Scale modeling does not only implies the

capacity of designing and operating large plants but also the skill of developing new and more efficient reaction technologies that would be cost and product quality competitive and meet environmental requirements [80].

CLC is a novel combustion technology that could capture CO_2 inherently with very little energy penalty. Research on scale modeling of CLC would significantly benefit the commercialization of this technology. However, scale-up of fluidized bed reactors is known to be more difficult than that of other types of reactors [83]. This difficulty is because of the complicated fluidization state inside the reactor and the many possible operating parameters. The history of fluidization scale-up has examples of success [84-86]; but severe failures have also been reported [83, 87]. Even today, the scale-up of fluidized bed technology is challenging [87]. In other words, just as Matsen [88] stated, 'scale-up is still not an exact science, but is rather a mix of physics, mathematics, witchcraft, history and common sense that we call engineering'.

Development and commercialization of any new chemical process will cost significant amount of time and effort, and requires substantial capital expenditures. Using proven techniques based on experience and mathematic and/or design models can minimize the risk and uncertainty when scaling up fluidized bed technology [89]. Currently, no open literature studies are known that have studied CLC reactor scale-up based on scaling laws.

2.7 Objectives

In this study, we will examine the development of novel OCs by using small amounts of CeO_2 as an additive to a Fe_2O_3 based OC. The objectives of this study are:

(1) To understand the reactivity of iron oxide based OCs by using TGA-MS and a bench scale CLC experiment setup;

(2) To investigate the effects of CeO_2 additive on particles' physical properties (morphology, BET surface area, mechanical strength);

(3) To elucidate and then discuss the mechanisms of the promoting role of CeO_2 in Fe_2O_3 based OC;

(4) To obtain the kinetic parameters of OCs;

(5) To perform a scale-up study of a CLC bench scale reactor, and to gain experience and insight on CLC fluidized bed reactors during scale-up, and to find potential correlations that would be beneficial for future CLC reactor scale-up.

3. Experimental

3.1 Oxygen carrier

Commercially available metal oxides were used during OC preparation. Aluminum oxide powder (Sigma-Aldrich, standard grade), iron oxide (Sigma-Aldrich, 99.0 % purity) and cerium oxide (Strem Chemicals, 99.9 %) were used to prepare OC materials by freeze granulation methods. Typically, a slurry was prepared by ball milling mixtures of metal oxides, dispersant (A40) and binder (PVA) within de-ionized water. The well-mixed slurry was sprayed through a nozzle into liquid nitrogen, leading to the formation of frozen spherical particles which were then dried in a freeze dryer (Virtis Advantage Plus). After freeze drying, the particles were calcined in air at 1400 ^{o}C for 6 hours. Three types of OC, labeled as OC #1, OC #2 and OC #3, were produced for this study, as shown in Table 4. The OCs were selected with a diameter between 150-300 μm.

3.2 Microscopic imaging

The morphology of the OC particles was examined using a Hitachi S-4800 scanning electron microscope. The OC particles were immobilized on the sample stage with conductive double sided carbon tape. The accelerating voltage was set to 15 kV.

3.3 Mechanical strength

The mechanical strength was measured in a Shimpo FGE-10X instrument which can record the peak force every time a particle was crushed. The mechanical strength was obtained by averaging 30 measurements using particles that had been randomly extracted from samples and having a particle size distribution range of the reaction tested samples (150-300 μm).

Table 4 Composition and sintering temperature of OCs

OC	Composition	Sintering Temperature
#1	10 wt. % CeO_2, 40 wt. % Al_2O_3, 50 wt. % Fe_2O_3	1400^oC
#2	50 wt. % Fe_2O_3, 50 wt. % Al_2O_3	1400^oC
#3	10 wt. % CeO_2, 90 wt. % Fe_2O_3	1400^oC

3.4 Surface area measurement

A Micromeritics ASAP 2020 surface analyzer was employed to examine microstructure of the OC samples. The surface area is based on the Brunauer-Emmett-Teller (BET) method. About 450 mg sample was used for each measurement. The sample was degassed at 160 ^oC for overnight, and then it was subjected to the isothermal measurement by N_2 adsorption-desorption at 77 K.

3.5 XRD

In order to investigate the crystalline phase of the samples, the X-ray diffraction patterns were obtained using a Rigaku SmartLab system in the 2 theta range of 20-90^o with CuKα irradiation.

3.6 Raman spectroscopy

Raman spectroscopy (Horiba-Jobin Yvon LabRam HR) was used to investigate the molecular speciation of the OCs in their oxidized and reduced forms. Spectral resolution was approximately 2 cm^{-1}; wavenumber calibration was checked using the silica vibrational mode at 520.7 cm^{-1}.

3.7 TGA/MS measurement

The CLC reaction testing included the use of a TGA-MS system (Netzsch STA449C and Netzsch QMS 403C) and a bench-scale CLC setup. The TGA-MS system is shown in Figure 3; in it was placed about 500 mg (±1 mg) of OC and then the OC was alternately oxidized or reduced using O_2 or CO diluted in argon, respectively. Mass flow controllers (MFCs) were used to control the flow rate of the feed gases and a LabView program was designed and used to control and monitor the MFCs. The redox cycles followed a sequence of: (i) 5 min argon purge at 200 ml min^{-1}; (ii) 20 min oxidation with 20 vol. % O_2 balanced with argon, at 200 ml min^{-1}; (iii) 5 min argon purge at 200 ml min^{-1}; and (iv) 30 min reduction with 20 vol. % CO balanced with argon, at 200 ml min^{-1}. The exhaust gas from the TGA was analyzed by mass spectrometry (MS) operated in a MID (multiple ion detection) mode.

3.8 Bench scale CLC setup

This bench scale test platform can provide not only important information for the performance of the OCs under realistic conditions as exist in commercial scale units, but also provide the experience for further scale-up and troubleshooting. Its diagram is presented in Figure 4. It was comprised of a single fixed bed reactor of 5 cm inner diameter, and was used to simulate the oxidation and reduction of a CLC system by use of a switching valve that alternately enabled either oxidizing or reducing gas into the bottom of the reactor. During each test about 100 g of the OCs were placed onto a height-adjustable distributor at the bottom of reactor; the bed height of the OCs was approximately 7.5 cm. A K-type thermocouple was immersed into the center of the OC bed. Based on preliminary testing, it was determined that a 5 l min^{-1} flow rate of feed gas

was appropriate to obtain a desired fluidization state. A Rosemond X-stream infrared multi-channel gas analyzer was used to measure the composition (O_2, CO, CO_2 and CH_4) of off-gas from the reactor. The experimental equipment used during reactor testing was controlled and data collected (temperature and gas concentrations) via a specially-designed LabView program. The furnace temperature can be set up to 1200 ^oC.

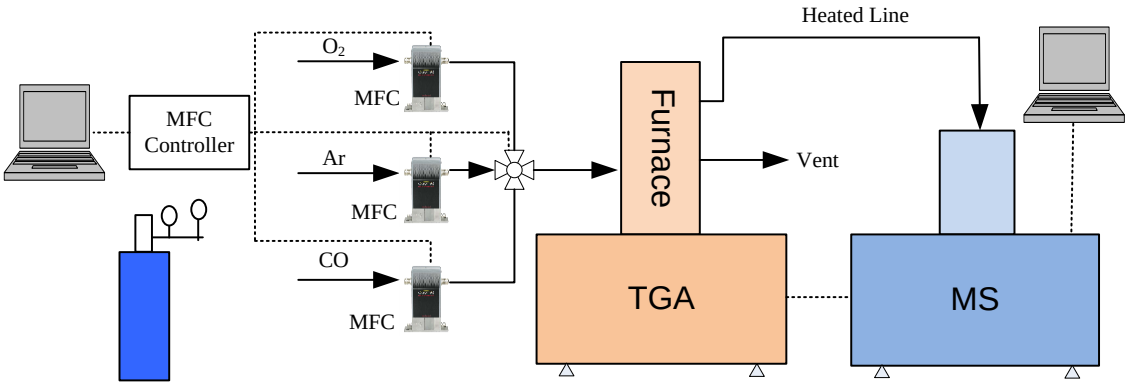

Figure 3 TGA-MS system.

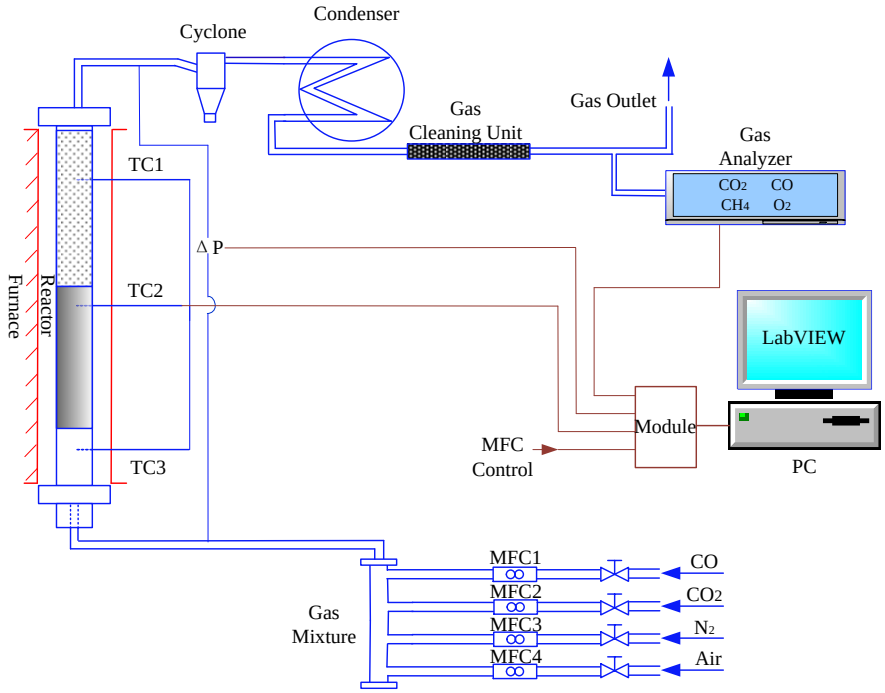

Figure 4 Bench scale CLC setup.

4. Reactivity Study

4.1 Effect of CeO_2 additive on the physical properties

The effect of CeO_2 on the physical properties of Fe_2O_3-based OCs was investigated first. Specifically, OC #1 and OC #2 particles were characterized by SEM, BET surface area and mechanical strength data acquisition. The SEM images of OC #1 and OC #2, presented in Figure 5**,** show that the OCs had very similar morphologies. The particles are spherical with a homogeneous, smoothed grain structure.

The BET surface area data of both OCs are shown in Figure 6. They had very small surface areas (0.34 $m^2 g^{-1}$ for freshly-calcined OC #1 and 0.31 $m^2 g^{-1}$ for freshly-calcined OC #2) typical of that caused by high temperature sintering. Upon being subjected to 5, 10 and 15 redox cycles, the surface areas were increased to 1.6 $m^2 g^{-1}$ but insignificant differences were found between the values for OC #1 and OC #2. Based on these data it was concluded that the addition of CeO_2 did not appreciably affect morphologies or surface areas of the OCs.

Structural properties can be further examined by carrying out mechanical strength measurements. Mechanical strength data of freshly-calcined OCs and after 5, 10 and 15 redox cycles are shown in Figure 7. Their mechanical strengths were identical, within the measurement uncertainties. Furthermore, mechanical strength did not change upon redox cycling. Hence, it is concluded that the addition of CeO_2 did not affect the OCs' mechanical strength.

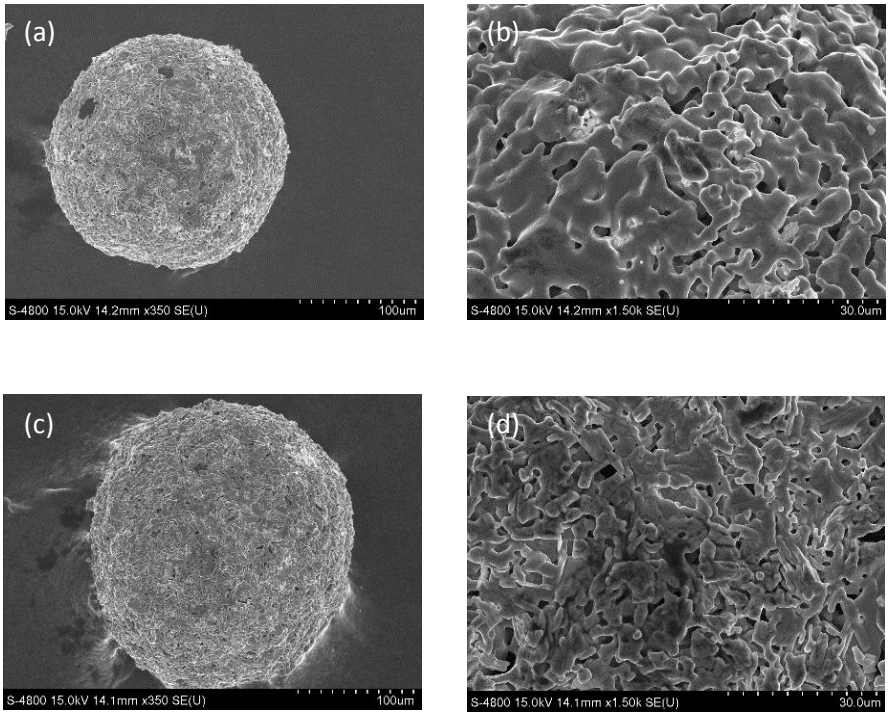

Figure 5 SEM images; (a) OC #1, 350; (b) OC #1, 1.5k; (c) OC #2, 350; (d) OC #2, 1.5k. The accelerating voltage was set to 15 kV, current was 20 μA.

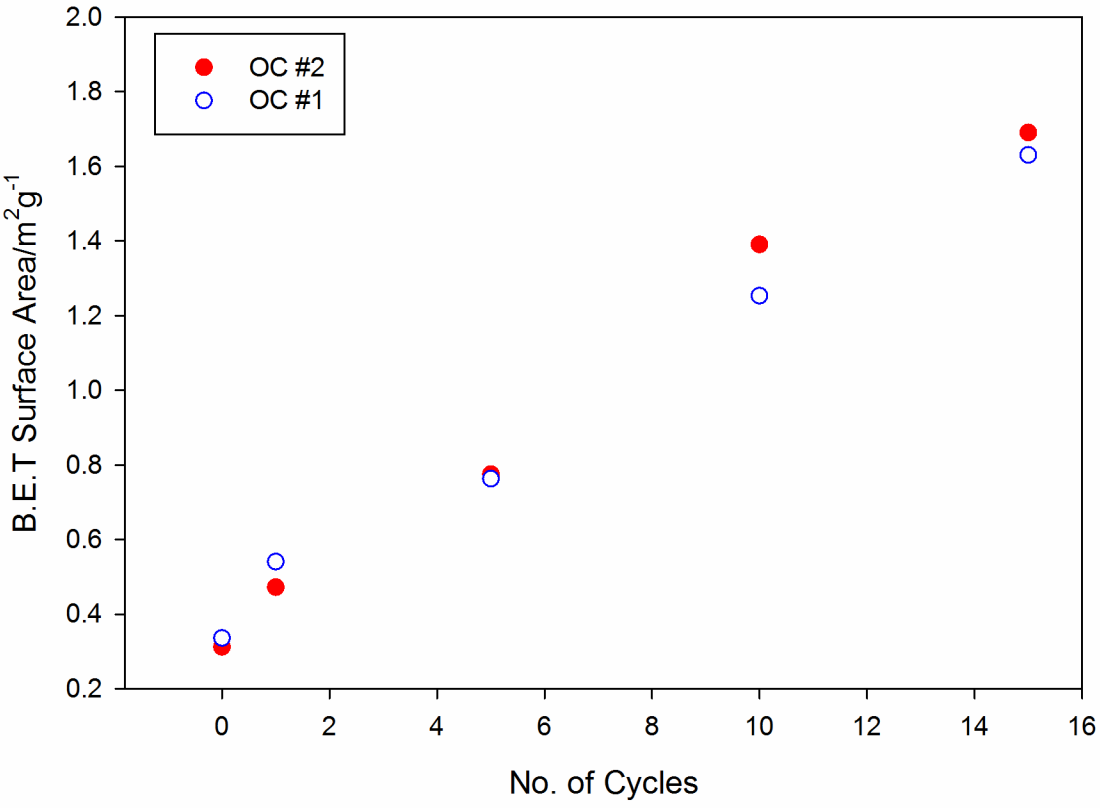

Figure 6 BET surface area.

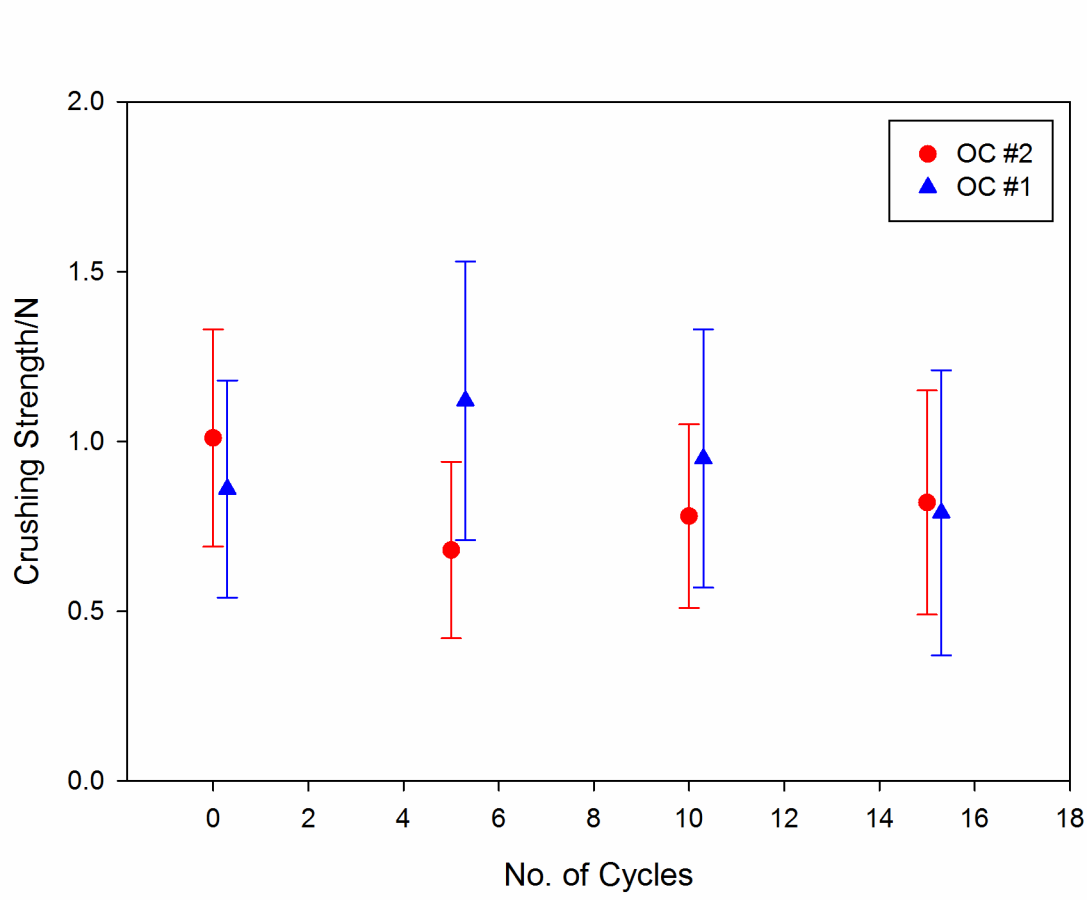

Figure 7 Mechanical strength.

4.2 Reactivity

The TGA-MS system and the bench-scale CLC reactor were used to investigate redox reactivity of the OC particles. Because oxidation reactivity is usually much faster than reduction reactivity, the reduction reactivity was the primary focus of this study. Before testing of the OCs, the TGA response baseline (without any samples) was measured to determine if fluctuations in apparent weights occurred during the switching between redox gas compositions. Also, although Al_2O_3 is usually considered an inert support, its weight loss was tested under the redox gases to measure if any weight loss or addition occurred during gas composition changes. Because CeO_2 can be partially reduced, it was necessary to prepare a reference sample of CeO_2 and Al_2O_3 and then to measure its weight loss or gain during redox cycling. The composition of this reference sample was 10 wt. % CeO_2 and 90 wt. % Al_2O_3, and was prepared following the OC production procedures and conditions described in the foregoing description. During each test, the reactivities were evaluated by averaging reaction rates over a 30 minute reaction exposure.

Determination of the baseline data was identical to that used for the OCs, with four steps during each cycle: purge, oxidation, purge and reduction, using the same flow rates and gas compositions. These baseline test results are shown in Figure 8. Nine redox cycles were used during the TGA baseline testing, the results of which were very consistent. In general, these TGA data showed only minor perturbations when the gas composition was switched, and this perturbation was repeatable. In contrast, the OC baselines were conducted for 20 redox cycles, the data from which were also very consistent and repeatable. Although it was anticipated that CeO_2 could lose oxygen during reduction at

high temperature, only a 0.1 % weight loss was measured for the OCs after the TGA baseline data were deducted. Hence, oxygen loss from CeO_2 is projected to be very limited and CeO_2 by itself could not be used as a main oxygen supplier during CLC.

The averaged reaction rate of OC #1 and OC #2 are shown in Figure 9 after the baseline was subtracted. Typical to these types of materials, several redox cycles were necessary to activate the OCs [42, 90], as can be seen in the reaction rate data in which five redox cycles for OC #1 and nine cycles for OC #2 were necessary before a constant and repeatable reaction rate occurred during each cycle. From Figure 9 it is evident that the OC with 10 % CeO_2 additive had better average reaction rate than did the other OC which was 7.7% higher than that of OC #2.

Figure 10 shows O_2 and CO_2 intensities from MS data during the 10^{th} redox cycle for OC #1, OC #2 and baseline (no sample); higher current signals correspond to higher gas concentrations. During reduction (part III), both OC#1 and OC #2 produced about 10 times greater CO_2 current intensity than the baseline testing. At the beginning of reduction, the CO_2 concentrations from both OCs were very close; this response could be caused by a similar availability of surface oxygen on the OCs because both OCs had the same concentration of Fe_2O_3, and the same particle sizes and surface areas. Although after several minutes of reaction the CO_2 concentrations from both OCs decreased below their concentrations at the beginning, the rate of change was different for both OCs such that the CO_2 concentration from OC #1 was higher than from OC #2. This difference continued to be magnified throughout the reduction cycle, a trend which would not be expected if both OCs had equal reaction efficiencies or equal oxygen availabilities. If most of the surface oxygen was consumed during the first minutes into the reduction,

then only bulk oxygen would be sustaining CO_2 production, and it would have to diffuse to the surface from the bulk of the OC to oxidize the CO. Furthermore, a decrease of CO_2 concentrations from both OCs would be expected after minutes into the reduction because bulk diffusion of oxygen and then reaction with CO is slower than the consumption of surface oxygen for CO oxidation. Hence, the higher CO_2 concentration from OC #1 than from OC #2 suggests that OC #1 provided faster oxygen transfer than did OC #2. This conclusion is consistent with the TGA results that OC #1 lost more weight than did OC #2 during reduction, and with the fact that more time was needed for the O_2 signal to stabilize during oxidation of OC #1 (part I, Figure 10). The result also suggests that reduced OC #1 absorbed more oxygen into the bulk than did OC #2.

However, the possibility exists that differences in CO_2 concentrations were the result of oxygen release from CeO_2 when at high temperature. To assess this possibility, both OCs were completely oxidized and then the gas was switched from oxidation conditions to inert conditions (part II, Figure 10). The MS data clearly show no O_2 signal differences between the two OCs and the baseline testing. Hence, no or inappreciable amounts of oxygen was released from CeO_2, a result which is consistent with Hedayati et al's research [71].

Figure 11 presents gas concentration data obtained during the reduction of the OCs within the bench-scale reactor. The data shows that CO_2 concentrations rose faster for both OCs, and the OCs had the ability to convert CO to CO_2 during the first three minutes; during the first four minutes OC #1 converted about 9.5 % more CO to CO_2 than did OC #2. These results suggest that OC #1 had a faster oxygen transfer rate and supplied more

oxygen for CO oxidation than did OC #2, a difference that is in agreement with the TGA-MS data.

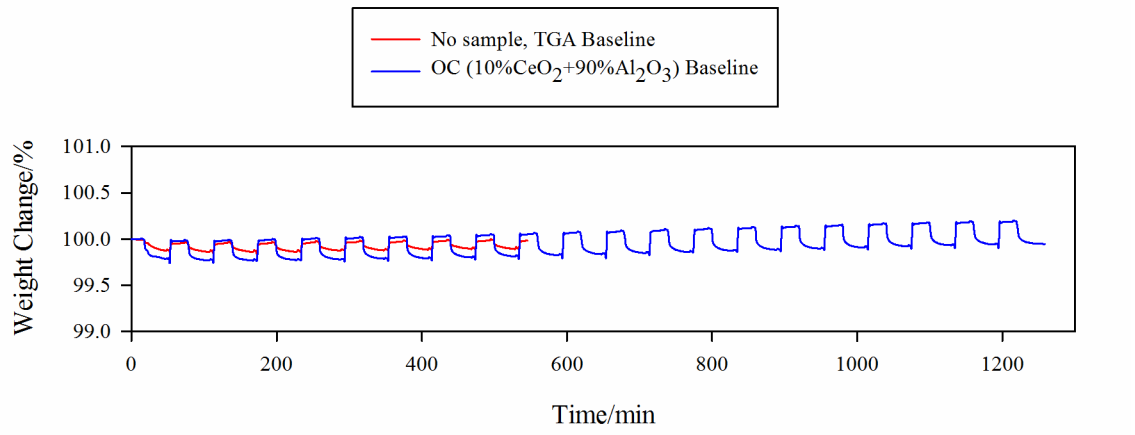

Figure 8 TGA results of baselines. The temperature was 950°C, and each redox cycle follows the sequence of purge, oxidation, purge and reduction. The reducing gas was 20 vol. % CO in argon.

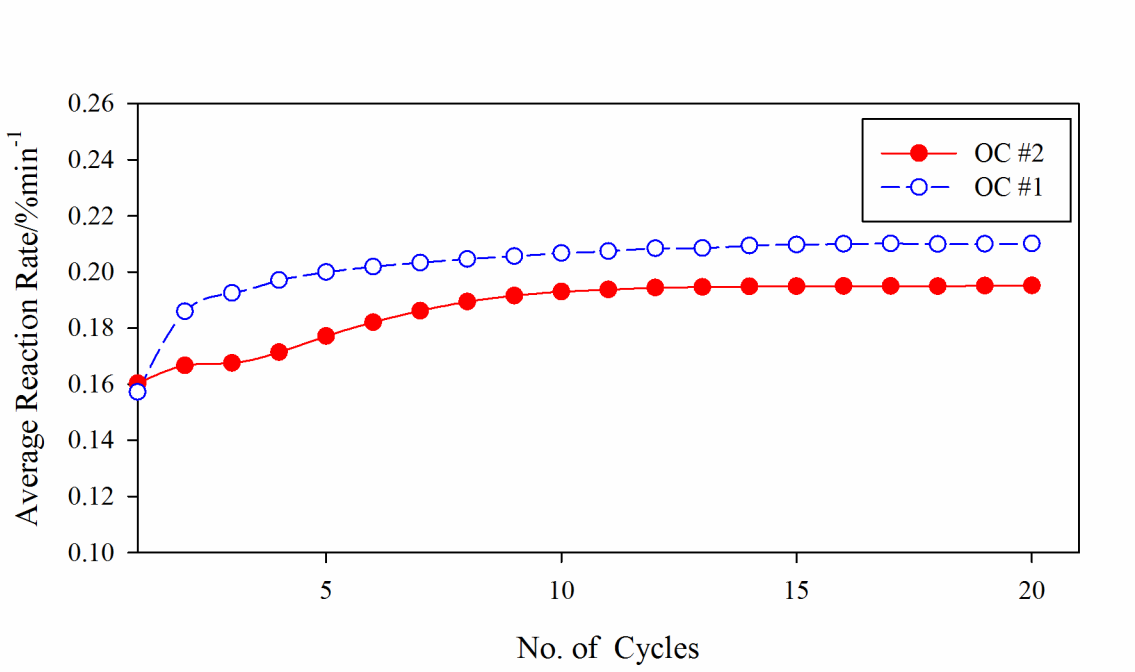

Figure 9 Comparison of average reaction rate. The temperature was 950°C, and each redox cycle follows the sequence of purge, oxidation, purge and reduction. The reducing gas was 20 vol. % CO in argon.

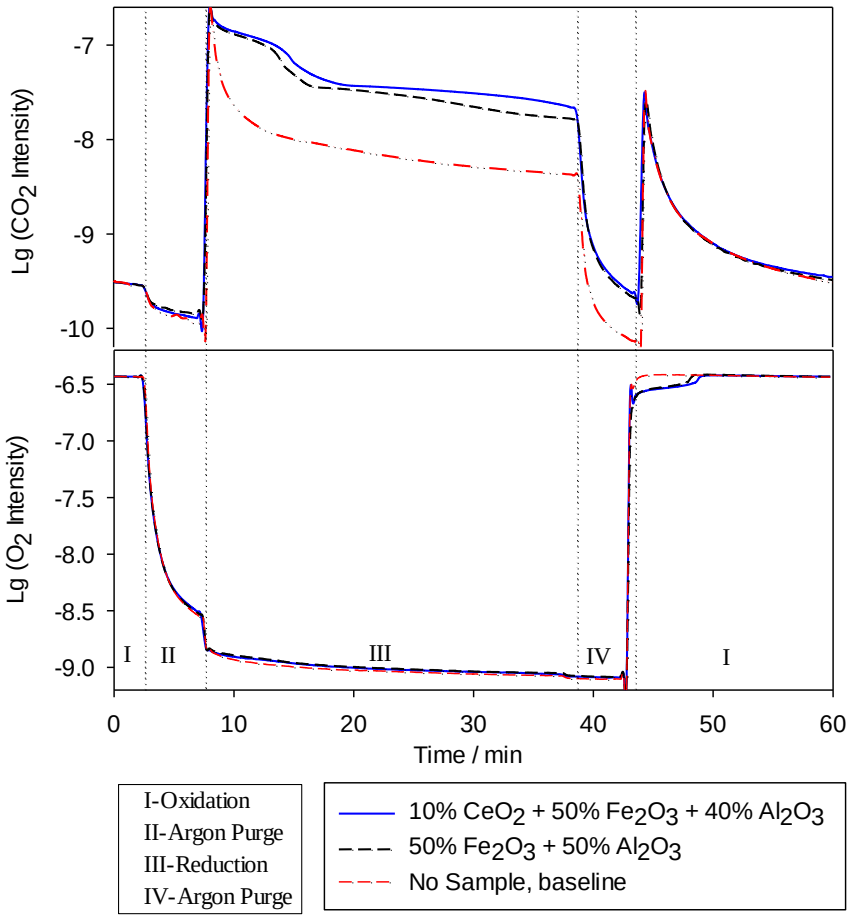

Figure 10 MS measurement, the y axis was expressed in logarithm.

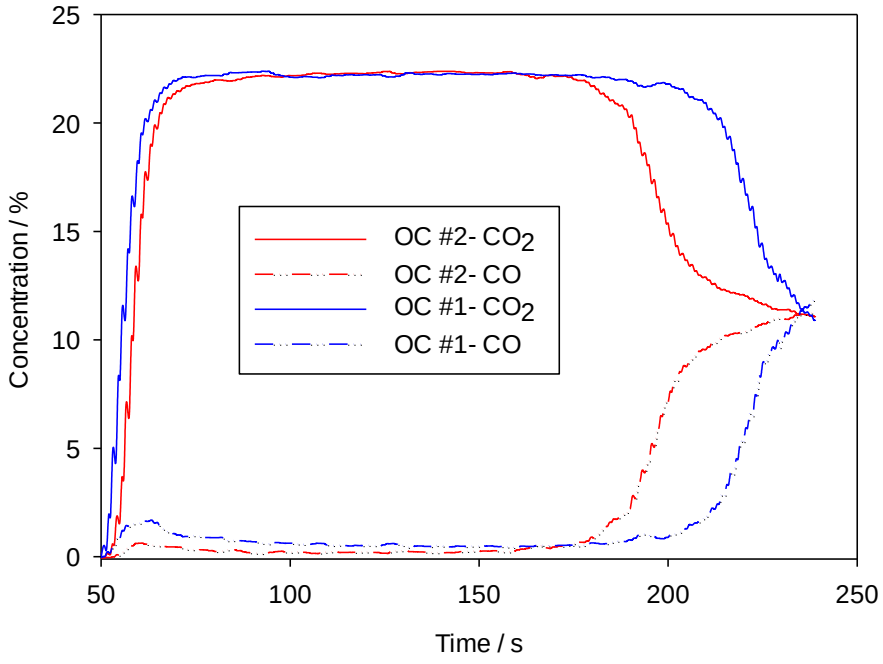

Figure 11 Gas concentrations from bench scale experiment. The temperature was 950^{o}C, and the reducing gas was 23 vol. % CO with argon.

4.3 Reaction mechanism

Bi-metal oxide-based OCs usually give better performance than mono-metal oxides [53], the dissimilarity of which has been attributed to "synergistic effects". Although this terminology is generic in nature, it has entailed different mechanisms depending on the metal oxide mixtures tested. To explore possible "synergistic effects" for the CeO_2-containing oxides in the current study, analytical examinations of the OCs were conducted to elucidate their chemical structure before and after exposure to oxidation and reduction conditions.

XRD data from the OCs and standard Fe_2O_3 and CeO_2 are presented in Figure 12. The results for oxidized OC #1 in comparison to the reference compounds point to Fe_2O_3 and CeO_2 moieties, but the OC #1 peaks are much broader which indicates a poorly crystallized or microcrystalline phase, or the presence of micro-strain [91]. To examine chemical structures that may provide mutual effects on the Fe_2O_3 and CeO_2 crystallinity, Raman spectra were obtained from the OCs in their oxidized and reduced forms, the results of which are shown in Figure 13. The vibrational bands of OC #1 in its oxidized state are similar in position to those of α-Fe_2O_3 (217, 283, 398, 488, 600) [92] and dissimilar in intensity to the Raman bands of OC #2. This comparison suggests that CeO_2 has influenced the bulk phase, possibly forcing OC #1 into a highly disordered α-Fe_2O_3–like phase.

To further examine structural differences between the OCs and possible reasons for the differences, XRD and Raman data were also acquired for reduced OC #1 (Figure 12 and Figure 13). Reduced OC #1 possesses Raman bands at 463, 608, and 694 cm^{-1}; the sharp

band at 463 cm^{-1} is similar in position to that of crystalline CeO_2 [93], while bands at 608 and 694 cm^{-1} are not indicative of a known phase. The only iron oxide phases that would exhibit vibrational modes in the 600-700 cm^{-1} region are FeO (650 cm^{-1}) and Fe_3O_4 (300, 520, 660 cm^{-1}) [92]. The spectrum has a small shoulder above the 463 cm^{-1} band at about 500 cm^{-1}, which could be related to distorted Fe_3O_4, possibly influenced by the presence of Ce in the bulk. Indeed, the XRD results show Fe_2O_3 reduction creates Fe_3O_4, FeO, Fe and $FeCeO_3$. This last component is identified according to the study by Ameta et al [94], and strongly suggests a solid state reaction between Fe_2O_3 and CeO_2 occurred during redox exposures. Therefore, it can be reasonably inferred that Fe_2O_3 and CeO_2 in OC #1 have formed a solid solution to some extent. Accordingly, and in consideration of: i) the CeO_2 content was only 10 wt. % of OC #1; and ii) its addition significantly improved the reaction performance of the OC #1, it is hypothesized that the structure of OC #1 became a mixture of Fe_2O_3 and Fe_2O_3-CeO_2 in solid solution during the redox processing. As a result, the synergistic effect of Fe_2O_3 with CeO_2 in solid solution along with Fe_2O_3 dramatically improved the reaction performance of OC #1.

It is well known that CeO_2 at high temperature or in the reduced state will lose a small amount of oxygen and, thereby, generate oxygen vacancies, as defined by:

$$2CeO_2=Ce_2O_3+O^* \quad (8)$$

Even in pure CeO_2, oxygen vacancies have been detected [93]. One more important fact was that doping low valence Fe^{3+} to CeO_2 will further increase the oxygen vacancy concentration. From this perspective, Fe_2O_3 exerts an influence on CeO_2.

The TGA-MS results show that oxygen species on the OC surfaces are quickly consumed by fuel; however, after the surface oxygen is consumed it is necessary for diffusion of bulk oxygen to the surface if CO oxidation is to continue. This diffusion would entail a "hopping" motion of the atoms because the crystal lattice restricts the positions and migration paths of atoms [95]. If vacancies are generated, the least energetic path for oxygen diffusion would involve continual occupation of nearby vacancies until the oxygen is consumed at the surface. For example, data have shown that oxygen diffusion through vacancies is 10^4 faster than through the lattice [96].

The potential of iron oxide to provide oxygen for fuel oxidation is high, about 30 % from Fe_2O_3 to Fe. The rate of fuel oxidation has been the problem – low rates mean long reaction times, high OC inventory and expensive CLC processing. If oxygen from Fe_2O_3 could be transferred through the oxygen vacancy generated by cerium oxides, oxygen transfer rates will be greatly increased. The TGA-MS and bench scale tests confirm that, the addition of CeO_2 could help the transfer of oxygen from the bulk to the surface. The formation of Fe_2O_3-CeO_2 solid solution could provide this prerequisite. If so, three types of oxygen transfer could exist in this solid solution: (1) by lattice diffusion; (2) by vacancy diffusion, in which an oxygen atom could jump to a neighboring vacancy. Oxygen vacancies maybe adjacent to each other to form an oxygen transfer tunnel, so oxygen could transfer from the inside to outside only from the oxygen transfer tunnel at a very fast speed; and (3) by lattice diffusion and vacancy diffusion.

Bhavsar et al [69] proposed a mechanism of the interaction between CeO_2 and NiO. The OC chosen by the author was NiO on the support of the reducible CeO_2. The author hypothesized the mechanism as: NiO on the surface of the OC was first reduced to

metallic Ni, then the Ni aided the cracking of CH_4 to C and H_2, then CeO_2 on the metal/support interface began to provide lattice oxygen, and finally the reduced oxygen depleted cerium oxide was replenished from the core partially oxidized NiO. Our study of iron oxide-based OC with CeO_2 have shown that OC #1 and OC #2 had very similar performance at the beginning of the reduction reaction, whereas after this initial reactivity, the oxygen transfer rate of OC #1 became larger than that of OC #2; the implications of this reactivity are significantly different than that proposed by Bhavsar et al [69] because, in that case, CeO_2 reacted with CH_4 at the beginning. Furthermore, our experiments show that CeO_2 has very limited oxygen transfer capacity itself. However, Bhavsar et al's [69] oxygen transfer mechanism is also partially supported in that CeO_2 could transfer oxygen from a partially reduced core NiO to the surface, which in our study was related to the formation of a Fe_2O_3 and CeO_2 solid solution; the solid solution should be an important step for interaction between Fe_2O_3 and CeO_2. In other words, a solid solution enables interaction of the oxygen during the reduction with not only at the surface of the metal/support interface but also throughout the whole particle.

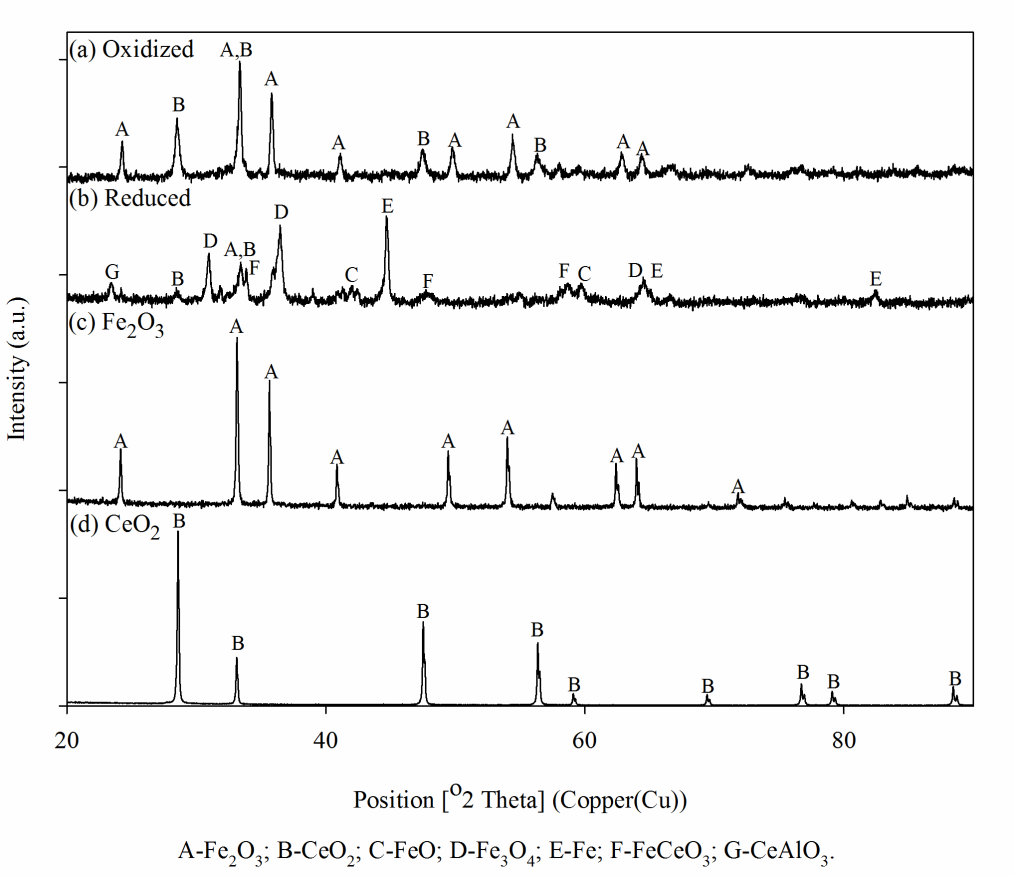

Figure 12 XRD spectra. The OC particles was crushed to fine powders before sent to the XRD test, the test was in the 2 theta range of 20^{o}-90^{o} with CuKα irradiation.

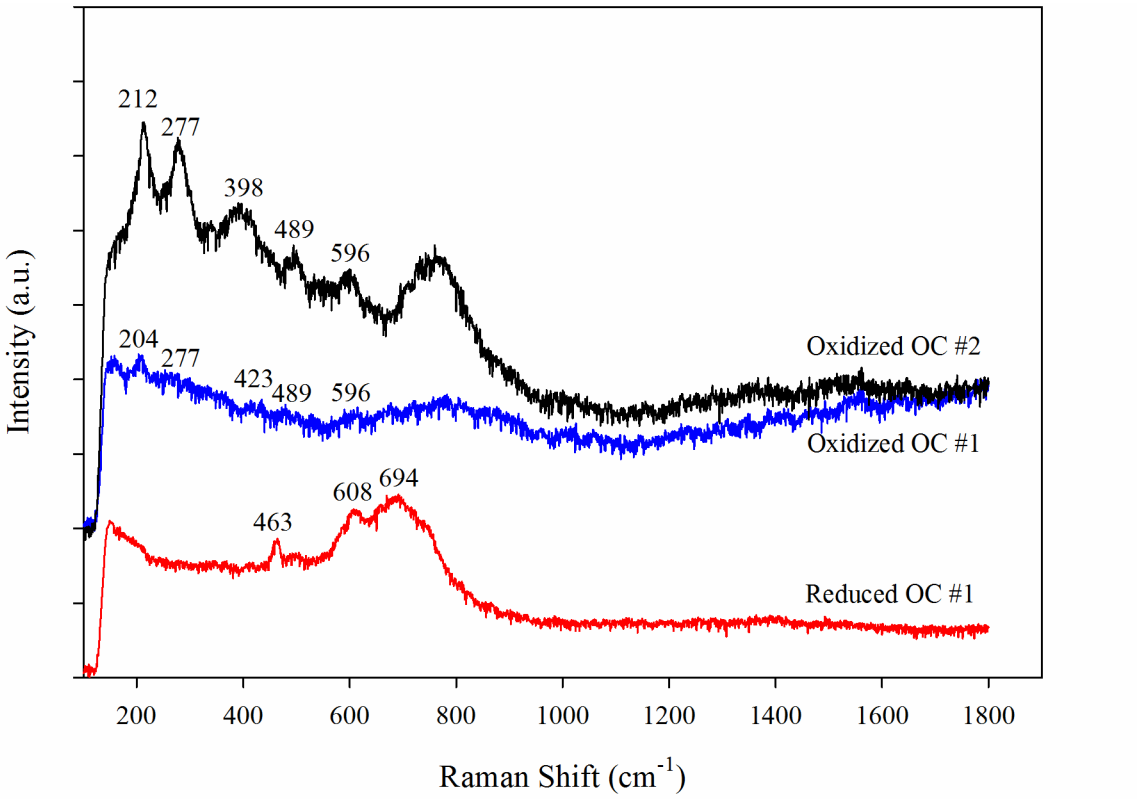

Figure 13 Raman spectra.

4.4 Reaction kinetics study

4.4.1 Shrinking core model (SCM)

The shrinking core model was used to carry out a kinetics analysis because a granulated structure was observed in the OC particles (Figure 5). Typically, the shrinking core model is useful in describing the reaction kinetics with this type of particle morphology [35]. The basic equation for the shrinking core model can be expressed as [97]:

$$w = dX_r/dt = 3(1 - X_r)^{2/3} kC^n \quad (9)$$

Where the terms are defined as: X_r -conversion, in %, *t*-time, in s, *k*-reaction rate constant, for reaction order of n, the unit is in $L^{n-1}\,mol^{1-n}\,s^{-1}$, *C*-reacting gas concentration, in mol L^{-1}, and *n*- reaction order.

Integration yields:

$$1 - (1 - X_r)^{1/3} = kC^n t \quad (10)$$

The reaction rate, *k*, according to Arrhenius law is expressed as:

$$k = Aexp(-E_a/RT) \quad (11)$$

Where the terms are defined as: *A*-pre-exponential factor, for reaction order of *n*, the unit is in $L^{n-1}\,mol^{1-n}\,s^{-1}$; E_a- activation energy, in J mol^{-1}, *R*-universal gas constant of 8.314 J $mol^{-1}K^{-1}$, and *T*-temperature, in K.

4.4.2 Results

The related reactions in this study are:

$$3Fe_2O_3 + CO \rightarrow 2Fe_3O_4 + CO_2 \quad (12)$$

$$Fe_2O_3 + CO \rightarrow 2FeO + CO_2 \quad (13)$$

$$Fe_3O_4 + CO \rightarrow 3FeO + CO_2 \quad (14)$$

$$FeO+CO \rightarrow Fe+CO_2 \quad (15)$$

As stated by Abad et al [98], the oxygen transferred to the fuel gas was a sum of the contribution of reduction of Fe_2O_3, Fe_3O_4 and FeO, so, in agreement, this reduction kinetics study is based on the global reduction reactions shown in Equations (12) to (15). Bench scale results for OC conversion involving different temperatures and CO concentrations are shown in Figure 14 and Figure 15. The CO concentration was kept constant while the temperature was varied, and the temperature was kept constant while the CO gas concentration was varied. The relationship between conversion and time in the figures indicates that the shrinking core model was appropriate [35].

For each reaction condition, the values of kC^n (slope of the line) can be found by curve fitting. By taking the logarithm of kC^n, a straight line with a slope of n is obtained, which is the reaction order. Since the CO concentration was known, the relationship of $\ln kC^n$ and $\ln C$ at three different CO concentrations was plotted, as shown in Figure 16. The slope of the fitted line was found to be 0.9 for OC #1 and 1.1 for OC #2. The reaction rate constant at specific temperatures can be acquired similarly.

A transformation of Arrhenius' law can be written as:

$$\ln(k) = \ln(A) + (-E_a/R)/T \quad (16)$$

By taking the Arrhenius plot, as shown in Figure 17, the activation energy and pre-exponential factors were obtained and are summarized in Table 5. The resulting kinetic parameters for the OC #1 that reacted with CO are: reaction order n=0.9, activation energy E_a=24.2 $\times 10^3$ J mol^{-1} and pre-exponential factor A=0.006 L$^{-0.1}$ mol$^{0.1}$ s^{-1}, and for OC #2 these parameters are: reaction order n=1.1, activation energy E_a=22.4 $\times 10^3$ J mol^{-1} and pre-exponential factor A=0.003L$^{0.1}$ mol$^{-0.1}$ s^{-1}. The values for these OC#1 and OC #2

are very close, possibly because these two OCs had similar physical properties and also because kinetics studies focus on performance at the beginning of a reaction when both OCs had the same reactivity. Hence, it is probable that the differences in their reactivities after depletion of surface oxygen and the onset of faster oxygen diffusion for OC #1 was not measured in these kinetics studies.

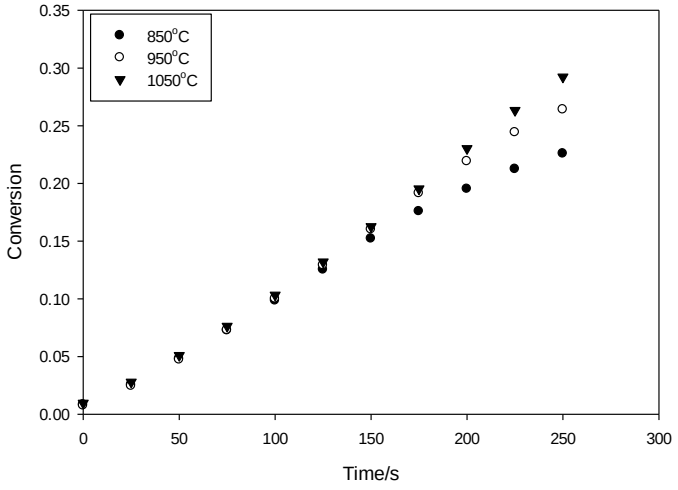

(a) OC #1

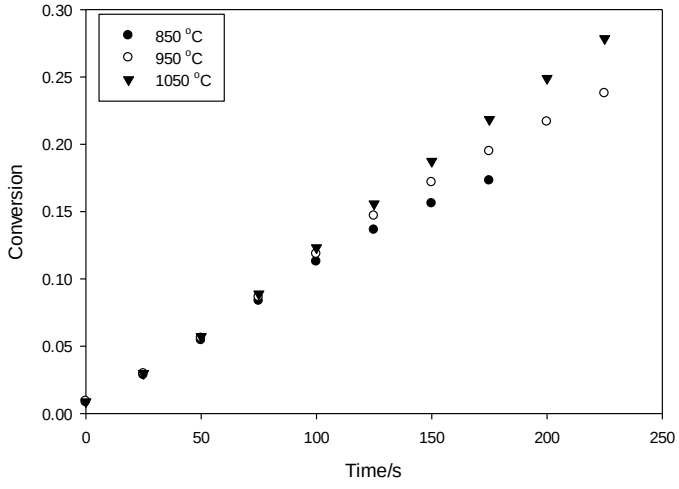

(b) OC #2

Figure 14 Temperature effect on conversion

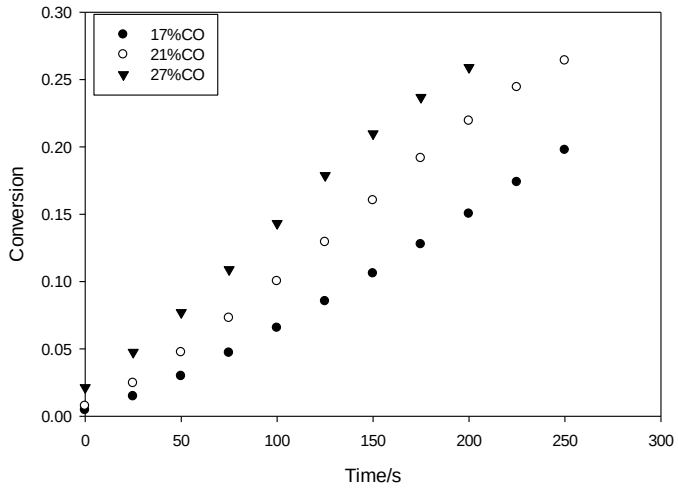

(a). OC #1

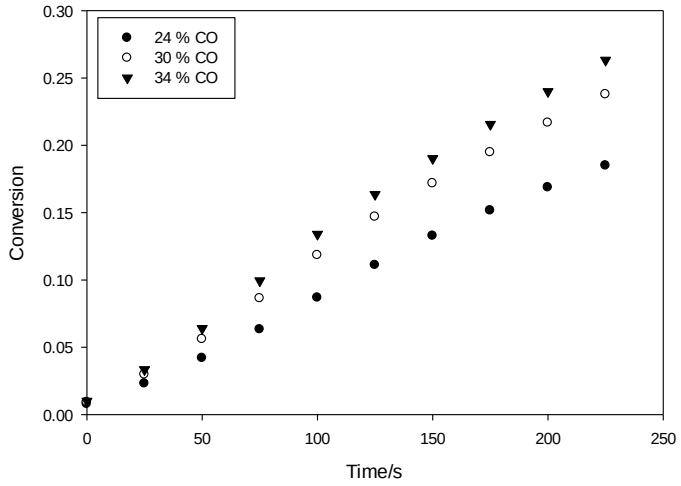

(b). OC #2

Figure 15 CO concentration effect on conversion

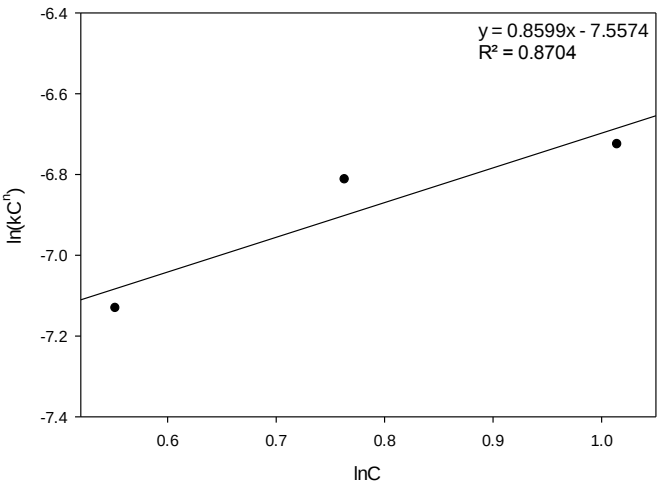

(a). OC #1

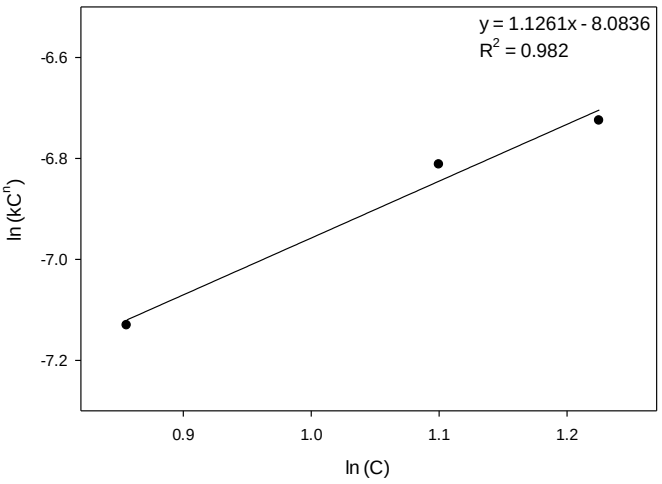

(b). OC #2

Figure 16 Plot of ln(kC^n) and ln(C)

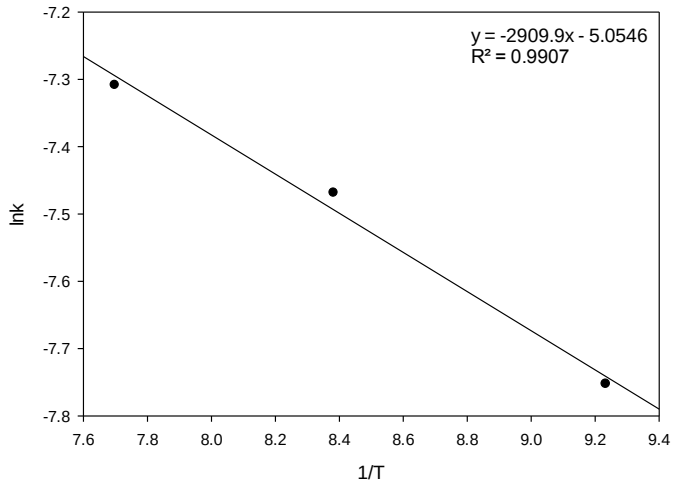

(a). OC #1

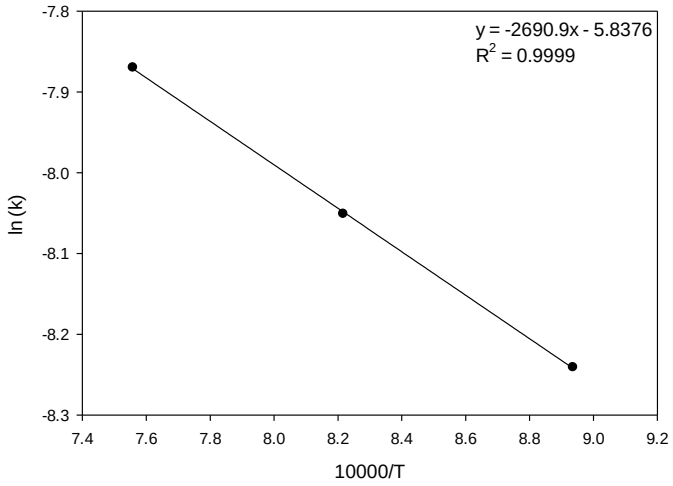

(b). OC #2

Figure 17 Arrhenius plot

Table 5 Kinetic parameters

Kinetic parameters	E_a	A	n
Unit	J mol^{-1}	L^{n-1} $mol1^{-n}$ s^{-1}	-
OC #1	24.2	0.006	0.9
OC #2	22.4	0.003	1.1

4.5 Conclusions

Iron-based OCs with and without CeO_2 additive were produced and physical properties such as morphology, surface area, and mechanical strength were investigated. The reactivity was tested by both TGA-MS and bench scale methods. The results for both OCs were compared and analyzed and the promotional role of CeO_2 was discussed. The following conclusions were drawn: (1) The addition of CeO_2 has no effect on the OCs morphology, BET surface area, or the mechanical strength; (2) Although OC #1 had higher reactivity than OC #2, this difference was not caused by differences in BET surface area or additional oxygen release from CeO_2 by itself; (3) The proposed promotional role of the CeO_2 is that it enables the creation of oxygen vacancies in a solid solution. These vacancies were able to transfer oxygen from Fe_2O_3 quickly to the surface of the OC by vacancy diffusion or through oxygen tunnel transfer. The formation of a CeO_2 and Fe_2O_3 solid solution provides the prerequisite for these short range interactions. (4) The kinetic parameters of both OCs are close to each other.

5. Scale-up Study

5.1 Governing equations

Mathematical modeling is the most basic approach to scale-up [81]. Anderson and Jackson [99] derived the governing equations for fluidized beds particles, these equations are as follows:

Global continuity equation:

$$\varepsilon_g + \varepsilon_s = 1 \tag{17}$$

Gas-phase continuity equation:

$$\frac{\partial \varepsilon_g}{\partial t} + \frac{\partial}{\partial x_i}\left(\varepsilon_g V_{gi}\right) = 0 \tag{18}$$

Solid-phase continuity equation:

$$\frac{\partial \varepsilon_s}{\partial t} + \frac{\partial}{\partial x_i}\left(\varepsilon_s V_{si}\right) = 0 \tag{19}$$

Gas-phase momentum equation:

$$\rho_g \varepsilon_g \left[\frac{\partial V_{gi}}{\partial t} + V_{gj}\frac{\partial V_{gi}}{\partial x_j}\right] = -\frac{\partial P}{\partial x_i} - \varepsilon_g \frac{\partial \tau_{ij}}{\partial x_j} - \beta(V_{gi} - V_{si}) \tag{20}$$

Solid-phase momentum equation:

$$\rho_s \varepsilon_s \left[\frac{\partial V_{sj}}{\partial t} + V_{sj}\frac{\partial V_{sj}}{\partial x_j}\right] = -\varepsilon_s \frac{\partial \sigma_{ij}}{\partial x_j} + \rho_s \varepsilon_s g_i + \beta(V_{gi} - V_{si}) \tag{21}$$

These equations can describe particles' movement very well, but they are too complicated to solve even with present computational means [81]. To successfully implement a scaling study it is therefore necessary to simplify these equations, one approach of which is to invoke hydrodynamic and chemical similarity by using sets of dimensionless numbers which have to be kept constant at both scales [87].

Glicksman [100] simplified the above governing equations and derived the scaling numbers by non-dimensionalizing these governing equations. They are called full set scaling laws and are as follows:

$$\frac{u_o \rho_g d_p}{\mu}; \frac{u_o^2}{gD}; \frac{\rho_g}{\rho_p}; \frac{D}{L}; \frac{d_p}{D}; \varphi; \Phi \tag{22}$$

However, using the full set of Glicksman scaling laws brings many constraints and is very difficult to implement [87]. To simplify the scaling laws and to make it easier to be implemented, we made the following assumptions: the governing forces in fluidized bed are inertia and buoyancy, and the viscous force is ignored, so viscosity is not important. Thus, it is reasonable to drop the Reynolds number. Furthermore, because this scale-up study is based on a hot model, it is necessary to add a dimensionless number reflecting the chemical reaction. The Damköhler number is a ratio of reaction rate to transport rate. It is an important parameter for chemical reaction, so the Damköhler number was added to the scaling laws. As a consequence, the modified scaling laws are proposed as follows:

$$\frac{u_o^2}{gD}; \frac{\rho_g}{\rho_p}; \frac{D}{L}; \varphi; \Phi, \mathrm{Da} \tag{23}$$

The simplified scaling laws eliminate some constraints and give better flexibility in model design, which provide freedom to choose the diameter of the cold flow model without a need for exotic particles and pressures. Hence, in this study, the same oxygen carrier (OC #1) was used for both reactors. As mentioned before, the OC has a composition of 50 wt. % Fe_2O_3, 10 wt. % CeO_2 and 40 wt. % Al_2O_3, with a size range of 150-300 μm.

Improvement in the potential of combustion scaling is possible if important parameters can be kept identical in a test plant and in a full-scale plant to meet combustion similarity.

These parameters include bed temperature, total excess-air ratios, primary stoichiometry, fuel type, and bed material [81, 101]. An important parameter for combustion similarity is reactor performance as measured by fuel conversion, product distribution, temperature distribution and selectivity [102-104]. For this study, reactors were designed and the operating parameters chosen based on the simplified set of scaling laws; reactor performance in a hot model was the focus. Hot model performance can be used to reflect the fluidization state. Conversion and temperature changes during the reactor testing were chosen for validating the scaling laws.

5.2 Experimental

An important aspect of model experiments is to confirm the similarity between the original phenomena and the scale model counterpart [84, 105]. In this study, the bench scale CLC setup was modified to conduct experiments.

Two reactors, reactor-1 and reactor-2, were fabricated with the scale ratio r = 2, as shown in Figure 18. Similar to the simplified fluidized bed scaling laws, to build these two reactors, Horio [106] suggested that:

$$r = \frac{D^l}{D^s} = \frac{L^l}{L^s} \tag{24}$$

$$\sqrt{r} = \frac{u_{mf}^l}{u_{mf}^s} = \frac{(u_o - u_{mf})^l}{(u_o - u_{mf})^s} \tag{25}$$

Hence, the reactors were built to meet hydrodynamic similarity. They were operated at the same temperature and pressure and, as mentioned previously, the materials in the two reactors were from the same batch. In this study, the Da was defined as:

$$Da = \frac{k_v}{u_o/L} \tag{26}$$

It scales with $\sqrt{r}$. For scaling validation, the time in the two different reactors must be scaled by a factor of $\sqrt{r}$ [87], namely:

$$\sqrt{r} = \frac{Da^l}{Da^s} \tag{27}$$

$$\sqrt{r} = \frac{t^l}{t^s} \tag{28}$$

Based on the above equations, the reactors design and operating parameters were determined and are shown in Table 6.

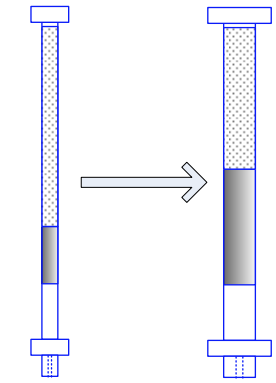

Figure 18 Two reactors.

Table 6 Reactor design and operate parameters

	D	L	M	Q	T	P	u_{mf}	k_v	Da
Units	mm	mm	g	L/min	^oC	bar	cm/s	s^{-1}	-
Reactor-1	25.4	3.81	12.5	2.8	970	1.0	2.6	0.00517	0.0022
Reactor-2	50.8	7.62	100	16	970	1.0	4.5	0.00520	0.0030

5.3 Results and discussion

In this study, the validation parameters were monitored by using the LabView program and by recording data every 0.5 seconds were the fuel conversion during reduction and temperature changes. The conversion χ was calculated by:

$$\chi = \frac{c_{CO_2}}{c_{CO}+c_{CO_2}} \tag{29}$$

These χ values-versus-time, presented in Figure 19 for both reactors, were very close to each other. At the beginning of the reaction, the OC induced high conversion because ample amounts of surface oxygen were available to convert CO into CO_2. However, as the reaction proceeded, the amount of oxygen available from the OC became less and less and led to a decrease in conversion. The conversion values decreased because oxygen was being supplied from the bulk of the OC, a process slower than oxygen transfer from the surface. Hence, for these reactors at a time greater than about 25 seconds, the conversion was controlled by oxygen diffusion from the bulk to the surface of the OC. Overall, the close match of conversion between reactor 1 and reactor 2 validates the scaling laws that were used.

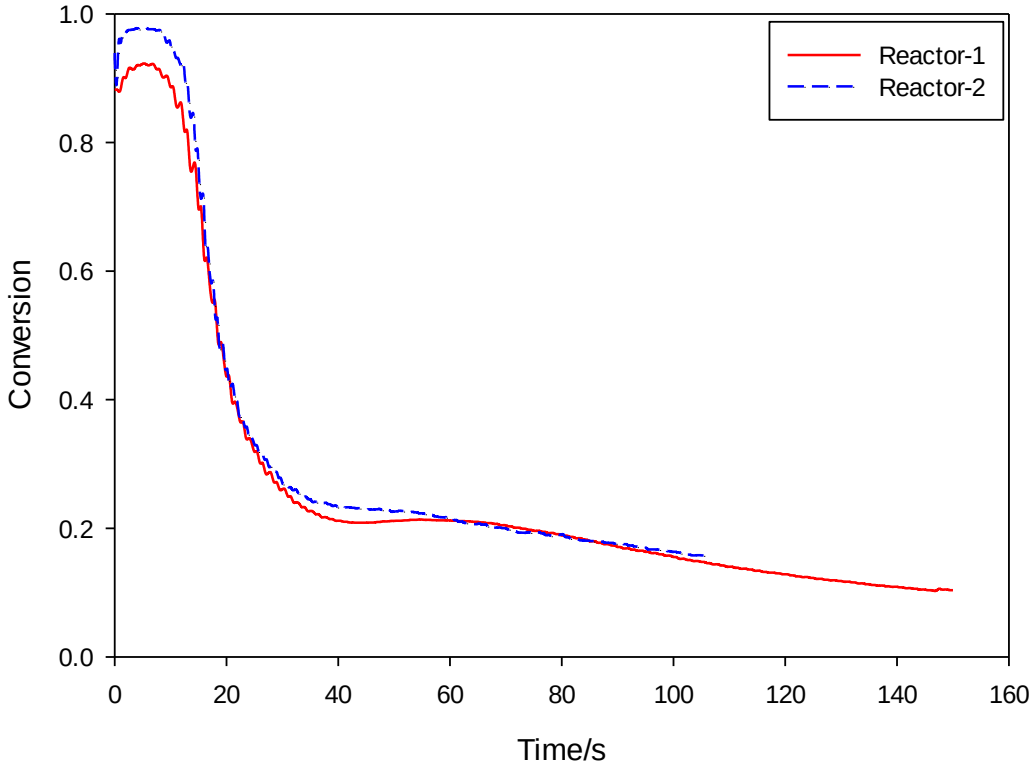

Figure 19 CO conversion.

Figure 20 shows the trends in temperature changes during the reduction reaction within the two reactors were very similar. Although not exactly identical, the temperature differences between the two reactors were very small compared to high temperature used during the testing. Temperature increases were noticed for both reactors because the reactions were exothermic, as shown in Table 3. Hence, the data confirms that appropriate scaling laws were used.

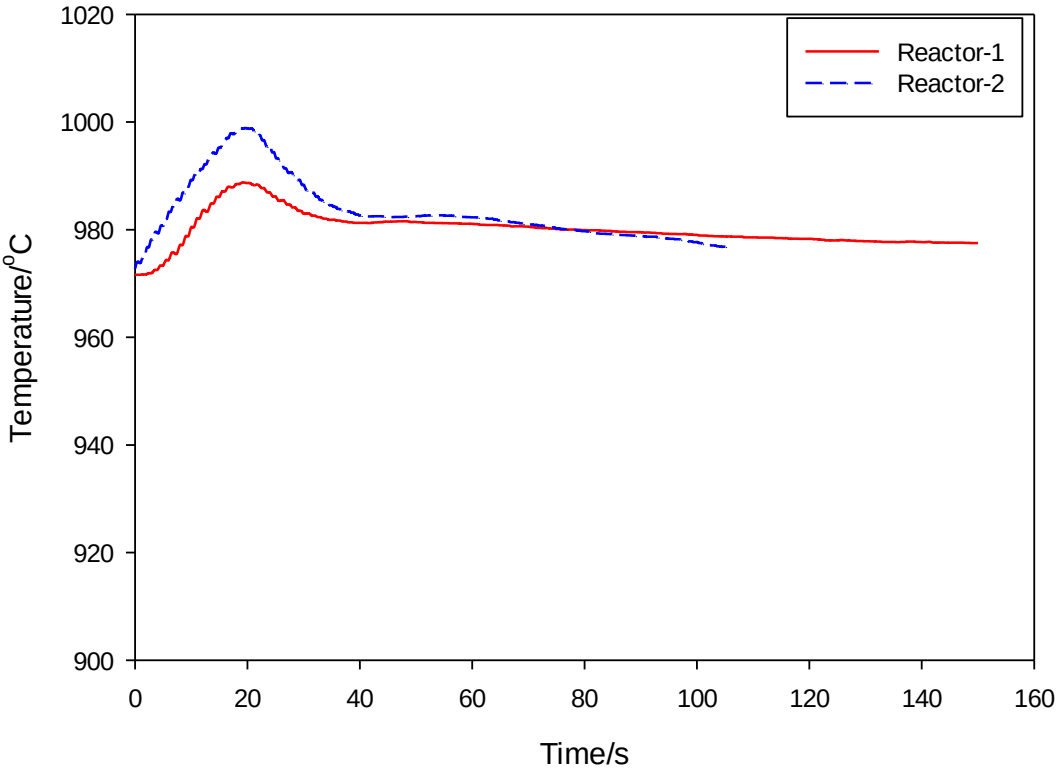

Figure 20 Temperature change.

5.4 Conclusions

Scaling laws of fluidized bed were applied to CLC reactors. Two CLC reactors with different size were built, as guided by scaling laws to meet hydrodynamic similarity, and then tested. Combustion similarity was the focus of this study and was monitored by acquiring and analyzing fuel conversion and temperature changes during the CLC reaction process. Comparison of conversion and temperature changes showed excellent combustion similarities in the two reactors, thereby validating the scale modeling method and the scale laws for CLC in fluidized beds. These results suggest the possibility for using scaling laws to scale-up even larger CLC reactors in the future.

6. Conclusions and Future Work

There is a general consensus on the need to reduce emissions of CO_2 from industrial process to limit or slow climate change resulting from increasing greenhouse gas concentrations in Earth's atmosphere. CLC has the advantages of in-situ oxygen separation, low NO_x emissions and low cost of CO_2 emission abatement. The use of CLC for power generation is an advanced energy technology that can capture CO_2 inherently, which could prove to be the next electricity generation technology in a carbon constrained future.

OC development and reactor scale-up are two important tasks for CLC technologies. Iron oxide based OCs, although suitable for CLC application, have less than optimum reactivity but embody attributes attractive for CLC and, hence, have attracted considerable research attention in recent years. Bi-metal oxide OCs usually impart better CLC performance than mono-metal oxide OCs. As a consequence, this dissertation focused on using CeO_2 as an additive to iron oxides based OCs to attempt to further improve reactivities.

Iron-based OCs with and without CeO_2 additive were produced and studied. The addition of CeO_2 had no effect on the OCs' morphology, BET surface area, or the mechanical strength. The reactivity at the surface of both OCs was close, and the kinetic parameters for both OCs were similar. Beyond the surface, OC with CeO_2 additive showed higher reactivity than OC without CeO_2. This difference was not caused by the BET surface area or an additional oxygen release from CeO_2 by itself. The proposed promotional role of CeO_2 additive is that it formed a solid solution with the iron oxide which enabled more

efficient diffusion through vacancy hopping or tunneling of bulk oxygen to the metal oxide surface where reduction and oxidation reactions occurred. The formation of the CeO_2-Fe_2O_3 solid solution was a prerequisite for improving the reactivity of the iron oxide OC.

Two CLC reactors with different size were built, guided by scaling laws to meet hydrodynamic similarity. Combustion similarity, fuel conversion and temperature change, during the CLC reaction process was established. Comparison of these factors showed excellent similarities in the two reactors, thereby validating the scale modeling method and the scale laws for CLC in fluidized beds. These results suggest the possibility for using scaling laws to scale-up even larger CLC reactors in the future.

In the future, several research directions need to be further studied. One direction is to test the CeO_2 promoted OC toward solid fuels because solid fuels such as coal can be used as fuel in CLC, and not enough gaseous fuels are available for CLC to meet potential commercial power generation needs. Coal is still the main energy source for power generation in the U.S.A and is also a dominant fuel in the world. Furthermore, coal deposits are well understood and abundant, making coal lower price option for energy generation. Thus, it is necessary to study the performance of CeO_2 promoted OCs with coal. Coals from difference places, like Powder River Basin (PRB), Illinois and Kentucky have different compositions and their reactivities to CLC may also be different.

The second direction is to study the water vapor effect on the performance of OCs. When solid fuel is used as fuel, water vapor is usually used as the fluidizing gas, because water vapor will gasify the solid fuel to gaseous fuel (i.e. coal gasification with water vapor to

produce H_2 and CO). The emergence of water vapor will affect the OCs' performance. The effect of H_2O (v) needs to be figured out.

The third direction is to continue reactor scale-up studies. The ultimate goal of CLC research is to apply CLC technology for power generation, thus commercial scale CLC technologies will need to be studied. Starting from the bench scale reactor, and through the scale modeling method, it may be possible to scale up to pilot scale reactors, and then the pilot scale reactors can be further scaled up to commercial scale, during which time process improvements and sophistication may need to be added.

Nomenclature

A	Pre-exponential factor; for reaction order of n, the unit is $L^{n-1}\ mol^{1-n}\ s^{-1}$
C	Gas concentration; mol L^{-1}
D	Diameter, m
Da	Damköhler number
E_a	Activation energy, J mol^{-1}
g	Gravity, 9.8 m s^{-2}
H	Heat of formation, J mol^{-1}
L	Bed height, m
k	Reaction rate constant; for reaction order of n, the unit is $L^{n-1}\ mol^{1-n}\ s^{-1}$
m	Mass, grams
n	Reaction order
P	Pressure, pa
Q	Flow rate, L min^{-1}
R	Universal gas constant, 8.314 J mol^{-1} K^{-1}
R_o	Oxygen transport capacity; %
r	Scale ratio

T	Temperature, K
t	Time, s
u	Velocity, m s^{-1}
V	Vector velocity
w	Reaction rate, % s^{-1}
X	Conversion of reduction, %
ρ	Density, kg m^{-3}
ΔH	Heat of reaction/combustion, J mol^{-1}
$v_i^{'}$	Mole concentration coefficient of reactant
$v_i^{''}$	Mole concentration coefficient of product
τ_{ij}	Gas phase stress tensor
σ_{ij}	Solid phase stress tensor
ε	Volume fraction, %
μ	Dynamic viscosity, pa·s
β	Drag coefficient
φ	Sphericity
Φ	Particle size distribution
ε_H	Voidage

χ	Conversion, %

Subscripts

g	Gas phase
mf	Minimum fluidization
s	Solid phase
o	Superficial
ox	Oxidized state
red	Reduced state
p	Particle
r	Reduction

Superscripts

l	Big
o	Standard temperature, 298K
s	Small

References

1. Ottmar, E.; Ramón, P.-M.; Youba, S., IPCC, 2011: Renewable Energy Sources and Climate Change Mitigation. Cambridge University Press Cambridge, United Kingdom and New York, NY, USA., 2011.

2. Hossain, M. M.; de Lasa, H. I., Chemical-looping combustion (CLC) for inherent separations—a review. Chemical Engineering Science 2008, 63 (18), 4433-4451.

3. Ed, D.; Pieter, T. NOAA/ESRL. www.esrl.noaa.gov/gmd/ccgg/trends/.

4. Goldberg, D. S.; Lackner, K. S.; Han, P., Co-Location of Air Capture, Subsea floor CO_2 Sequestration, and Energy Production on the Kerguelen Plateau. Environmental Science & Technology 2013, 47 (13), 7521-7529.

5. Monastersky, R., Global carbon dioxide levels near worrisome milestone. Natural 2013, 497, 13-14.

6. Yu, H., Carbon Capture and Storage: A Challenging Approach for Mitigation of Global Warming. International Journal of Clean Coal and Energy 2013, 2, 23-24.

7. Mathias, P. M.; Reddy, S.; Smith, A., Thermodynamic analysis of CO_2 capture solvents. International Journal of Greenhouse Gas Control 2013, 19, 262-270.

8. Adánez, J.; de Diego, L. F.; García-Labiano, F., Selection of Oxygen Carriers for Chemical-Looping Combustion. Energy & Fuels 2004, 18 (2), 371-377.

9. US Department of Energy, N. DOE/NETL Carbon Dioxide Capture and Storage RD&D Roadmap; 2010.

10. Padurean, A.; Cormos, C.-C.; Agachi, P.-S., Pre-combustion carbon dioxide capture by gas–liquid absorption for Integrated Gasification Combined Cycle power plants. International Journal of Greenhouse Gas Control 2012, 7, 1-11.

11. Jenni, K. E.; Baker, E. D.; Nemet, G. F., Expert elicitations of energy penalties for carbon capture technologies. International Journal of Greenhouse Gas Control 2013, 12, 136-145.

12. Jones, D.; Bhattacharyya, D.; Turton, R., Optimal design and integration of an air separation unit (ASU) for an integrated gasification combined cycle (IGCC) power plant with CO_2 capture. Fuel Processing Technology 2011, 92 (9), 1685-1695.

13. Emadi, A.; Sohrabi, M.; Jamiolahmady, M., Reducing heavy oil carbon footprint and enhancing production through CO_2 injection. Chemical Engineering Research and Design 2011, 89 (9), 1783-1793.

14. Granite, E. J.; O'Brien, T., Review of novel methods for carbon dioxide separation from flue and fuel gases. Fuel Processing Technology 2005, 86 (14-15), 1423-1434.

15. Herzog., H.; Eliasson., B.; O. Kaarstad, Capturing greenhouse gases. Scientific American 2000, 282 (2), 72-79.

16. Marion., J.; Nsakala., N. y.; Griffin., T. In Controlling Power Plant CO_2 Emissions: A Long Range View, Conference Proceedings Power Gen Europe, Europe, 2001.

17. Fang, H.; Haibin, L.; Zengli, Z., Advancements in Development of Chemical-Looping Combustion: A Review. International Journal of Chemical Engineering, 2009.

18. Brandvoll, O.; Bolland, O., Inherent CO_2 Capture Using Chemical Looping Combustion in a Natural Gas Fired Power Cycle. Journal of Engineering for Gas Turbines and Power 2004, 126 (2), 316-321.

19. Naqvi, R.; Bolland, O.; Brandvoll, O., Chemical Looping Combustion-Analysis of Natural Gas Fired Power Cycles With Inherent CO_2 Capture. ASME Conference Proceedings 2004, 301-309.

20. Wolf, J.; Anheden, M.; Yan, J., Comparison of nickel- and iron-based oxygen carriers in chemical looping combustion for CO_2 capture in power generation. Fuel 2005, 84 (7-8), 993-1006.

21. Wolf, J.; Yan, J., Parametric study of chemical looping combustion for tri-generation of hydrogen, heat, and electrical power with CO_2 capture. International Journal of Energy Research 2005, 29 (8), 739-753.

22. Consonni, S.; Lozza, G.; Pelliccia, G., Chemical-Looping Combustion for Combined Cycles With CO[sub 2] Capture. Journal of Engineering for Gas Turbines and Power 2006, 128 (3), 525-534.

23. Naqvi, R.; Wolf, J.; Bolland, O., Part-load analysis of a chemical looping combustion (CLC) combined cycle with CO2 capture. Energy 2007, 32 (4), 360-370.

24. Liu, K. Solid-Fueled Pressurized Chemical Looping with Flue-Gas Turbine Combined Cycle for Improved Plant Efficiency and CO_2 Capture 2012.

25. Mattisson, T.; Lyngfelt, A.; Cho, P. In Possibility of using iron oxide as an oxygen carrier for combustion of methane with removal of CO_2 — application of chemical-looping combustion, Fifth international conference on greenhouse gas control technologies, Cairns, Australia, Cairns, Australia, 2000.

26. Mattisson, T.; Lyngfelt, A.; Cho, P., The use of iron oxide as an oxygen carrier in chemical-looping combustion of methane with inherent separation of CO_2. Fuel 2001, 80 (13), 1953-1962.

27. Cho, P.; Mattisson, T.; Lyngfelt, A., Comparison of iron-, nickel-, copper- and manganese-based oxygen carriers for chemical-looping combustion. Fuel 2004, 83 (9), 1215-1225.

28. Ishida, M.; Takeshita, K.; Suzuki, K., Application of Fe_2O_3−Al_2O_3 Composite Particles as Solid Looping Material of the Chemical-Loop Combustor. Energy & Fuels 2005, 19 (6), 2514-2518.

29. Zafar, Q.; Mattisson, T.; Gevert, B., Redox Investigation of Some Oxides of Transition-State Metals Ni, Cu, Fe, and Mn Supported on SiO_2 and $MgAl_2O_4$. Energy & Fuels 2005, 20 (1), 34-44.

30. Son, S. R.; Kim, S. D., Chemical-Looping Combustion with NiO and Fe_2O_3 in a Thermobalance and Circulating Fluidized Bed Reactor with Double Loops. Industrial & Engineering Chemistry Research 2006, 45 (8), 2689-2696.

31. Abad, A.; García-Labiano, F.; de Diego, L. F., Reduction Kinetics of Cu-, Ni-, and Fe-Based Oxygen Carriers Using Syngas (CO + H_2) for Chemical-Looping Combustion. Energy & Fuels 2007, 21 (4), 1843-1853.

32. Fan, L. S. Chemical Looping Technology and CO_2 Capture. http://gcep.stanford.edu/pdfs/KPjZOQnaKgBFZIEyZD_d-Q/LSFan.pdf.

33. Xiao, R.; Song, Q.; Zhang, S., Pressurized Chemical-Looping Combustion of Chinese Bituminous Coal: Cyclic Performance and Characterization of Iron Ore-Based Oxygen Carrier. Energy & Fuels 2009, 24 (2), 1449-1463.

34. Zhang, Y.; Liu, F.; Chen, L., Investigation of the Water Vapor Influence on the Performance of Iron-, Copper-, and Nickel-Based Oxygen Carriers for Chemical Looping Combustion. Energy & Fuels 2013, 27 (9), 5341-5351.

35. Liu, F.; Zhang, Y.; Chen, L., Investigation of a Canadian Ilmenite as an Oxygen Carrier for Chemical Looping Combustion. Energy & Fuels 2013, 27 (10), 5987-5995.

36. Law, C. K., Combustion Physics. Cambridge University Press; 1 edition, 2010.

37. NIST, NIST-JANAF Thermochemical Tables.

38. Leion, H.; Jerndal, E.; Steenari, B.-M., Solid fuels in chemical-looping combustion using oxide scale and unprocessed iron ore as oxygen carriers. Fuel 2009, 88 (10), 1945-1954.

39. Leion, H.; Mattisson, T.; Lyngfelt, A., Use of Ores and Industrial Products As Oxygen Carriers in Chemical-Looping Combustion. Energy & Fuels 2009, 23 (4), 2307-2315.

40. Scott, S. A.; Dennis, J. S.; Hayhurst, A. N., In situ gasification of a solid fuel and CO_2 separation using chemical looping. AIChE Journal 2006, 52 (9), 3325-3328.

41. Gu, H.; Shen, L.; Xiao, J., Chemical Looping Combustion of Biomass/Coal with Natural Iron Ore as Oxygen Carrier in a Continuous Reactor. Energy & Fuels 2010, 25 (1), 446-455.

42. Adánez, J.; Cuadrat, A.; Abad, A., Ilmenite Activation during Consecutive Redox Cycles in Chemical-Looping Combustion. Energy & Fuels 2010, 24 (2), 1402-1413.

43. Bidwe, A. R.; Mayer, F.; Hawthorne, C., Use of ilmenite as an oxygen carrier in chemical looping combustion-batch and continuous dual fluidized bed investigation. Energy Procedia 2011, 4, 433-440.

44. Kolbitsch, P.; Bolhàr-Nordenkampf, J.; Pröll, T., Operating experience with chemical looping combustion in a 120kW dual circulating fluidized bed (DCFB) unit. International Journal of Greenhouse Gas Control 2010, 4 (2), 180-185.

45. Berguerand, N.; Lyngfelt, A., The use of petroleum coke as fuel in a 10kW_{th} chemical-looping combustor. International Journal of Greenhouse Gas Control 2008, 2 (2), 169-179.

46. Berguerand, N.; Lyngfelt, A., Chemical-Looping Combustion of Petroleum Coke Using Ilmenite in a 10 kW_{th} Unit−High-Temperature Operation. Energy & Fuels 2009, 23 (10), 5257-5268.

47. Berguerand, N.; Lyngfelt, A., Batch testing of solid fuels with ilmenite in a 10kW_{th} chemical-looping combustor. Fuel 2010, 89 (8), 1749-1762.

48. Leion, H.; Lyngfelt, A.; Johansson, M., The use of ilmenite as an oxygen carrier in chemical-looping combustion. Chemical Engineering Research and Design 2008, 86 (9), 1017-1026.

49. Leion, H.; Mattisson, T.; Lyngfelt, A., Solid fuels in chemical-looping combustion. International Journal of Greenhouse Gas Control 2008, 2 (2), 180-193.

50. Cho, P.; Mattisson, T.; Lyngfelt, A., Carbon Formation on Nickel and Iron Oxide-Containing Oxygen Carriers for Chemical-Looping Combustion. Industrial & Engineering Chemistry Research 2005, 44 (4), 668-676.

51. Johansson, M.; Mattisson, T.; Lyngfelt, A., Investigation of Fe_2O_3 with $MgAl_2O_4$ for Chemical-Looping Combustion. Industrial & Engineering Chemistry Research 2004, 43 (22), 6978-6987.

52. Leion, H.; Mattisson, T.; Lyngfelt, A., The use of petroleum coke as fuel in chemical-looping combustion. Fuel 2007, 86 (12-13), 1947-1958.

53. Johansson, M.; Mattisson, T.; Lyngfelt, A., Creating a Synergy Effect by Using Mixed Oxides of Iron- and Nickel Oxides in the Combustion of Methane in a Chemical-Looping Combustion Reactor. Energy & Fuels 2006, 20 (6), 2399-2407.

54. Rydén, M.; Johansson, M.; Cleverstam, E., Ilmenite with addition of NiO as oxygen carrier for chemical-looping combustion. Fuel 2010, 89 (11), 3523-3533.

55. Marcus, J. Screening of oxygen-carrier particles based on iron-, manganese-, copper- and nickel oxides. Chalmers University of Technology, Göteborg, Sweden 2007.

56. Abad, A.; Mattisson, T.; Lyngfelt, A., The use of iron oxide as oxygen carrier in a chemical-looping reactor. Fuel 2007, 86 (7–8), 1021-1035.

57. Hossain, M. M.; de Lasa, H. I., Reduction and oxidation kinetics of Co–Ni/Al_2O_3 oxygen carrier involved in a chemical-looping combustion cycles. Chemical Engineering Science 2010, 65 (1), 98-106.

58. Adánez, J.; García-Labiano, F.; de Diego, L. F., Nickel−Copper Oxygen Carriers To Reach Zero CO and H_2 Emissions in Chemical-Looping Combustion. Industrial & Engineering Chemistry Research 2006, 45 (8), 2617-2625.

59. Lambert, A.; Delquié, C.; Clémeneçon, I., Synthesis and characterization of bimetallic Fe/Mn oxides for chemical looping combustion. Energy Procedia 2009, 1 (1), 375-381.

60. Ksepko, E.; Siriwardane, R.; Tian, H. In Effect of H_2S on chemical looping combustion of coal derived synthesis gas over Fe_2O_3-MnO_2 supported on ZrO_2/sepiolite., 1st Int Conf on Chemical Looping, Lyon, France, Lyon, France, 2010.

61. Shulman, A.; Cleverstam, E.; Mattisson, T., Manganese/Iron, Manganese/Nickel, and Manganese/Silicon Oxides Used in Chemical-Looping With Oxygen Uncoupling (CLOU) for Combustion of Methane. Energy & Fuels 2009, 23 (10), 5269-5275.

62. Hoteit, A.; Chandel, M. K.; Delebarre, A., Nickel- and Copper-Based Oxygen Carriers for Chemical Looping Combustion. Chemical Engineering & Technology 2009, 32 (3), 443-449.

63. Chandel, M. K.; Hoteit, A.; Delebarre, A., Experimental investigation of some metal oxides for chemical looping combustion in a fluidized bed reactor. Fuel 2009, 88 (5), 898-908.

64. Hoteit, A.; Chandel, M. K.; Durécu, S., Biogas combustion in a chemical looping fluidized bed reactor. International Journal of Greenhouse Gas Control 2009, 3 (5), 561-567.

65. Sayle, T. X. T.; Parker, S. C.; Catlow, C. R. A., Surface oxygen vacancy formation on CeO_2 and its role in the oxidation of carbon monoxide. J. Chem. Soc., Chem. Commun. 1992, 977-978.

66. Karlheinz, S., Materials design of solid electrolytes. PNAS 2006, 103 (10), 3497.

67. Campbell, C. T.; Peden, C. H. F., Oxygen Vacancies and Catalysis on Ceria Surfaces. Science 2005, 309 (5735), 713-714.

68. Trovarelli, A., Catalytic properties of ceria and CeO_2-containing materials. Catalysis Reviews-Science and Engineering 1996, (38), 439-520.

69. Bhavsar, S.; Veser, G., Reducible Supports for Ni-based Oxygen Carriers in Chemical Looping Combustion. Energy & Fuels 2013, 27 (4), 2073-2084.

70. Bhavsar, S.; Veser, G., Bimetallic Fe–Ni Oxygen Carriers for Chemical Looping Combustion. Industrial & Engineering Chemistry Research 2013.

71. Hedayati, A.; Azad, A.-M.; Rydén, M., Evaluation of Novel Ceria-Supported Metal Oxides As Oxygen Carriers for Chemical-Looping Combustion. Industrial & Engineering Chemistry Research 2012, 51 (39), 12796-12806.

72. Miller, D. D.; Siriwardane, R., Mechanism of Methane Chemical Looping Combustion with Hematite Promoted with CeO2. Energy & Fuels 2013.

73. Galvita, V.; Poelman, H.; Marin, G., Hydrogen Production from Methane and Carbon Dioxide by Catalyst-Assisted Chemical Looping. Topics in Catalysis 2011, 54 (13-15), 907-913.

74. He, F.; Wei, Y.; Li, H., Synthesis Gas Generation by Chemical-Looping Reforming Using Ce-Based Oxygen Carriers Modified with Fe, Cu, and Mn Oxides. Energy & Fuels 2009, 23 (4), 2095-2102.

75. Li, K.; Wang, H.; Wei, Y., Syngas Generation from Methane Using a Chemical-Looping Concept: A Review of Oxygen Carriers. Journal of Chemistry 2013, 8.

76. Li, K.; Wang, H.; Wei, Y., Direct conversion of methane to synthesis gas using lattice oxygen of CeO2–Fe2O3 complex oxides. Chemical Engineering Journal 2010, 156 (3), 512-518.

77. Sadykov, V. A.; Kuznetsova, T. G.; Alikina, G. M., Ceria-based fluorite-like oxide solid solutions as catalysts of methane selective oxidation into syngas by the lattice oxygen: synthesis, characterization and performance. Catalysis Today 2004, 93–95, 45-53.

78. Abanades, S.; Le Gal, A., CO_2 splitting by thermo-chemical looping based on $Zr_xCe_{1-x}O_2$ oxygen carriers for synthetic fuel generation. Fuel 2012, 102, 180-186.

79. Galvita, V. V.; Poelman, H.; Bliznuk, V., CeO_2-Modified Fe_2O_3 for CO_2 Utilization via Chemical Looping. Industrial & Engineering Chemistry Research 2013, 52 (25), 8416-8426.

80. Donati, G.; Paludetto, R., Scale up of chemical reactors. Catalysis Today 1997, 34 (3–4), 483-533.

81. Leckner, B.; Szentannai, P.; Winter, F., Scale-up of fluidized-bed combustion – A review. Fuel 2011, 90 (10), 2951-2964.

82. Kuwana, K.; Hassan, M. I.; Singh, P. K., Scale-model experiment and numerical simulation of steel teeming processes. SME Journal: Materials and Manufacturing Processes 2008, 23 (4), 1-6.

83. Werther, J., Scale-up modeling for fluidized bed reactors. Chemical Engineering Science 1992, 47 (9–11), 2457-2462.

84. Emori, R. I.; Saito, K.; Sekimoto, K., Scale Models in Engineering Gihodo Publishing Co.: Tokyo, 2008. In Japanese.

85. Saito, K., Progress in Scale Modeling: Summary of the First International Symposium on Scale Modeling (ISSM in 1988) and Selected Papers from subsequent Symposia (ISSM II in 1997 through ISSM V in 2006). Springer: 2008.

86. Kunii, D.; Levenspiel, O., Fluidization Engineering Butterworth-Heinemann; 2 edition, 1991.

87. Rüdisüli, M.; Schildhauer, T. J.; Biollaz, S. M. A., Scale-up of bubbling fluidized bed reactors — A review. Powder Technology 2012, 217, 21-38.

88. Matsen, J. M., Design and scale-up of CFB catalytic reactors. In Circulating Fluidized Beds, Grace, J. R.; Avidan, A. A.; Knowlton, T. M., Eds. Springer Netherlands: 1996; pp 489-503.

89. Knowlton, T. M.; Karri, S. B. R.; Issangya, A., Scale-up of fluidized-bed hydrodynamics. Powder Technology 2005, 150 (2), 72-77.

90. Schwebel, G. L.; Leion, H.; Krumm, W., Comparison of natural ilmenites as oxygen carriers in chemical-looping combustion and influence of water gas shift reaction on gas composition. Chemical Engineering Research and Design 2012, 90 (9), 1351-1360.

91. Pérez-Alonso, F. J.; López Granados, M.; Ojeda, M., Chemical Structures of Co-precipitated Fe−Ce Mixed Oxides. Chemistry of Materials 2005, 17 (9), 2329-2339.

92. de Faria, D. L. A.; Venâncio Silva, S.; de Oliveira, M. T., Raman microspectroscopy of some iron oxides and oxyhydroxides. Journal of Raman Spectroscopy 1997, 28 (11), 873-878.

93. Bao, H.; Chen, X.; Fang, J., Structure-activity Relation of Fe_2O_3–CeO_2 Composite Catalysts in CO Oxidation. Catalysis Letters 2008, 125 (1-2), 160-167.

94. Ameta, J.; Kumar, A.; Ameta, R., Synthesis and Characterization of $CeFeO_3$ Photocatalyst Used in Photocatalytic Bleaching of Gentian Violet. Journal of the Iranian Chemical Society 2009, 6, 293-297.

95. Mehrer, H., Diffusion in Solids. In Fundamentals,Methods,Materials, Diffusion-Controlled Processes, Ed.: Cardona, M.; Fulde, P.; Klitzing von K.; Queisser H.-J.; Springer: Berlin Heidelberg New York, 2007.

96. Tian, H.; Chaudhari, K.; Simonyi, T., Chemical-looping Combustion of Coal-derived Synthesis Gas Over Copper Oxide Oxygen Carriers. Energy & Fuels 2008, 22 (6), 3744-3755.

97. Moghtaderi, B.; Song, H., Reduction Properties of Physically Mixed Metallic Oxide Oxygen Carriers in Chemical Looping Combustion. Energy & Fuels 2010, 24 (10), 5359-5368.

98. Abad, A.; Adánez, J.; Cuadrat, A., Kinetics of redox reactions of ilmenite for chemical-looping combustion. Chemical Engineering Science 2011, 66 (4), 689-702.

99. Anderson, T. B.; Jackson, R., Fluid Mechanical Description of Fluidized Beds. Equations of Motion. Industrial & Engineering Chemistry Fundamentals 1967, 6 (4), 527-539.

100. Glicksman, L. R., Scaling relationships for fluidized beds. Chemical Engineering Science 1988, 43 (6), 1419-1421.

101. Leckner, B.; Werther, J., Scale-up of Circulating Fluidized Bed Combustion. Energy & Fuels 2000, 14 (6), 1286-1292.

102. Jazayeri, B., Successfully scale up catalytic gas-fluidized beds. Journal Name: Chemical Engineering Progress; Journal Volume: 91; Journal Issue: 4; Other Information: PBD: Apr 1995, Medium: X; Size: pp. 26-31.

103. Kelkar, V. V.; Ng, K. M., Development of fluidized catalytic reactors: Screening and scale-up. AIChE Journal 2002, 48 (7), 1498-1518.

104. Kimball, E. E.; Geerdink, P.; Goetheer, E. L., Scale-up of Fixed-Bed Chemical Looping Combustion. In Spring Meeting & 7th Global Congress on Process Safety, 2011.

105. Emori, R. I.; Saito, K., A Study of Scaling Laws in Pool and Crib Fires. Combustion Science and Technology 1983, 31 (5-6), 217-231.

106. Horio, M.; Nonaka, A.; Sawa, Y., A new similarity rule for fluidized bed scale-up. AIChE Journal 1986, 32 (9), 1466-1482.

Vita

Fang Liu

Born in Shan Dong Province, China

Education:

September 2003-July 2007 B.S. Thermal Engineering and Power Generation

September 2007-July 2010 M.S. Fluid Machinery and Engineering

September 2010-present Ph.D. Candidate, Mechanical Engineering

Professional Societies:

Combustion Institute, 2012-present

Certificate:

Lean Systems Student Certificate

Princeton-CEFRC Summer School on Combustion

Publications

Journals:

Liu, F.; Zhang,Y.; Chen, L.; Qian, D.; Neathery, J.; Saito, K.; Liu, K.; "Investigation of a Canadian Ilmenite as Oxygen Carrier for Chemical Looping Combustion"; Energy & Fuel, 2013. **27**(10): p. 5987-5995.

Liu, F.; Saito, K.; Liu K.; "Scale-up of Chemical Looping Combustion"; Springer, Progress in Scale Modeling, volume 2, 2014.

Liu, F.; Neathery, J.; Saito, K; Liu, K.; "CeO_2 Promoted Iron Based Oxygen Carrier for Chemical Looping Combustion"; submitted to the 35th International Symposium on Combustion.

Zhang,Y.; **Liu, F**.; Chen, L.; Han, C.; Neathery, N.; Liu, K.; " Investigation of Water Vapor Influence on the Performance of Iron, Copper and Nickel Based Oxygen Carriers for Chemical Looping Combustion", Energy & Fuel; 2013. **27**(9): p. 5341-5351.

Chen, L.; Zhang,Y.; **Liu, F**.; Neathery, N.; Liu, K.; "Development of cost-effective oxygen carrier from red mud for direct-coal-fueled chemical-looping combustion", submitted to Energy & Fuel.

Presentations/Proceedings:

Liu, F.; Li, T..; Neathery, J.; Liu, K.; Saito, K. "Characterization and Kinetic Study of Ilmenite for Chemical Looping Combustion," CSSCI (Central States Section of the Combustion Institute) April 22-24, Dayton, OH, 2012

Liu, F.; Zhang, Y.; Rubel, A; Neathery, J.; Liu, K. "Density, Particle Size Based Ash Separation from Oxygen Carrier and Char in Bench Scale Chemical Looping Combustion System"; 10th Annual Conference on Carbon Capture & Sequestration, May 2-5, Pittsburgh, Pennsylvania, 2011.

Liu, F.; Saito, K.; Liu K; "CO_2 Capture and Possible Impact on Painting"; Painting Technology Workshop, October 30-31, Lexington, Kentucky, 2012

Slone, J.; **Liu, F**.; Zhang, Y.; Rubel, A.; Neathery, J.; Liu, K.; " Characterization of Ilmenite for Chemical-Looping Combustion by Carbon Monoxide in a Bench-Scale

Fluidized Bed Reactor. " 2011 AIChE Annual meeting, Oct 16- 21; Minneapolis, MN, 2011.

Li, T.; **Liu, F**.; et al.; "An analysis of transient oxidation of magnetite to hematite in chemical looping combustion", ESSCI (Easter States Section of the Combustion Institute) Oct 13-16, Clemson, SC, 2013

Chen, L.; Zhang, Y.; **Liu, F**.; Han, C.; Neathery, J.; Liu, K.; " Development and Performance Evaluation of a Cost-effective Oxygen Carriers from Red Mud for Chemical Looping Combustion" 2012 AIChE Annual meeting, Oct 28–Nov 2, Pittsburgh, Pennsylvania, 2012